Middle East Journal of Applied Sciences
Volume: 14 | Issue: 01| Jan. – Mar. | 2024

EISSN: 2706 -7947 ISSN: 2077- 4613
DOI: 10.36632/mejas/2024.14.1.6
Journal homepage: www.curresweb.com
Pages: 72-100

Impact of Natural Synthesized Silver Nanoparticles on Soft Tissue Infecting Bacteria

Hadeer A. Salama [1], Mohamed M. Fathy[2], Mohammed Ezz El-din[1] and Doaa Ghaith[3]

[1]Botany and Microbiology Department, Faculty of Science, Cairo University, Egypt.
[2]Biophysics Department, Faculty of Science, Cairo University, Egypt.
[3]Clinical Pathology Department, Faculty of Medicine, Cairo University, Egypt.

Received: 20 Sept. 2023 **Accepted:** 15 Jan. 2024 **Published:** 10 Feb. 2024

ABSTRACT

This study includes the impact of some natural synthesized silver nanoparticles on soft tissue infecting bacteria (*Staphylococcus aureus, Pseudomonas aeruginosa, E. coli,* and *Klebsiella pneumoniae*). This study represents a simple, reliable, cost effective and green method for the synthesis of Ag NPs by treating silver ions with different concentrations of peel extract of *Citrus paradisi*, (1-Ag NPs, 2-Ag NPs, and 3-Ag NPs). Synthesized silver nano formulations were characterized by ultraviolet-visible absorption spectroscopy, dynamic light scattering (DLS), zeta potential and transmission electron microscopy (TEM). The antibacterial activity of Ag NPs was evaluated using a series of assays: well diffusion method, disc diffusion method, antibiotic susceptibility test, and microdilution method. The mean particle size of prepared silver nanoparticles are 19.76 nm, 16.99 nm and 5.89 nm for 1-Ag NPs, 2-Ag NPs, and 3-Ag NPs, respectively. The prepared silver nanoparticles inhibited all the tested organisms. The smallest nanoparticle size had the greatest inhibitory effect concerning to the other antimicrobial agent (antibiotics Polimixin B (PB) (300unit), Ciprofloxacin CIP (5µg), Tigecyclin TGC (15µg), Aztreonam AT(30µg), Cefepime FEP (30µg), Cefoxitin CX (30µg), Ceftriaxone CTR (30µg), Amoxicillin/Clavulanic acid AMC (30µg), Ceftazidime CAZ (30µg), Piperacillin/Tazobactam PIT (100/10µg), Imipenem IPM (10µg), Meropenem MRP (10µg), Amikacin AK (30µg), Co-Trimoxazole (Sulpha/Trimethoprim) COT (25µg), Ampicillin AMP (10µg), Gentamicin GEN (10µg), Ofloxacin OF (5µg), Levofloxacin LEV (5µg), Doxycycline Hydrochloride DO (30µg), Erythromycin E (15µg), Clindamycin CD (2µg), Vancomycin VA (30µg), Ampicillin/Sulbactam A/S (10/10 µg), Azithromycin AZM (15µg), Linezolid LZ (30µg), Cefaclor CF (30µg), Teicoplanin TEC (30µg), Cefuroxime CXM (30µg)). Some of tested bacteria (*Staphylococcus aureus*, *Pseudomonas aeruginosa*, and *E. coli*) were moderately sensitive except *Klebsiella pneumoniae* which was completely resistant. This point that the use of silver nanoparticles Ag NPs was the best favorable for control of *Klebsiella pneumoniae.* Concerning microdilution method, the result indicated the *Klebsiella pneumoniae* was the most inhibited bacteria with MIC concentration 0.047µg/mL and *Pseudomonas aeruginosa* the least inhibited bacteria with MIC concentration 0.19 µg/mL. Concerning transmission electron microscope TEM, the result indicated the tested bacteria *(Staphylococcus aureus*, *Pseudomonas aeruginosa)* showed wall rupture and extrusion of the cellular contents as consequence of adhesion of nanoparticles upon bacterial cell surface. These results suggest that Ag NPs could be used as an adjuvant for the treatment of soft tissue infection.

Keywords: Silver nanoparticles, Citrus paradisi, antimicrobial activity, *Staphylococcus aureus, Pseudomonas aeruginosa*, *E. coli, Klebsiella pneumoniae*, Antibiotics.

1. Introduction

The use of plants for the preparation of nanoparticles has gained more relevance in the past decade as the technique is simple and involves the use of plants extracts which contain biomolecules of medicinal value (Roy & Das, 2015). Nanoparticles synthesis in recent years has received considerable

Corresponding Author: Hadeer A. Salama, Botany and Microbiology Department, Faculty of Science, Cairo University, Egypt.

attention due to their special features and potential applications (Sathishkumar *et al.,* 2009). Silver, gold and other metal common nanoparticles, nanoclusters, nanowires and related nanostructures have received tremendous attention owing to their unique catalytic, electrical, magnetic and thermal properties. Nano silver has immense applications in the field of detection, diagnostics, therapeutics, and antimicrobial activity (Sachin *et al.,* 2012). Various chemical and physical methods have been developed to prepare silver nanoparticles (Ag NPs). Among them, the chemical reduction is the most widely used. These approaches are usually associated with the use of hazardous chemicals such as reducing agent, stabilizers, and organic solvent. These approaches are usually associated with the use of hazardous chemicals such as reducing agent, stabilizers, and organic solvents. This may also involve special requirements for the employed techniques such as high energy radiation and microwave irradiation (Rao & Tang, 2017). Many of these methods are either expensive or involve the use of harmful chemicals. Therefore, there is an increasing need to develop ecofriendly, non-toxic and cost-effective methods for the preparation of Ag NPs without the application of toxic chemicals and special equipment. Recently, the biological approach using microorganisms and plant extracts have become valuable alternatives to chemical synthesis (Jackson *et al.,* 2018).

AgNPs, along with other nanomaterials, have been studied in the defined post-antibiotic era to search for new agents that can help combat pathogenic microorganisms without promoting the appearance of new resistances (Betts *et al.,* 2018). As an antibiotic alternative, this application has been broadly studied in recent years with the objective of developing new bactericidal products for decontamination or infection treatments taking advantage of the already established knowledge about their efficiency even against multidrug resistant organisms (Lee *et al., 2019)*.

Skin and soft tissue infections (SSTIs) are a common reason for consultations in primary health care centers. They are clinical entities with varying manifestations, etiologies, and severities, ranging from mild to life-threatening infections. They involve microbial invasion of the skin layers and soft tissues, followed by a process that leads to clinical effects as a result of the interaction between microorganisms and host defenses. SSTIs can be caused by various microorganisms, mainly bacteria and fungi (Moffarah *et al., 2016;* Clebak *et al.,* 2018; Amparo *et al., 2020).*

Due to the increase in strains resistant to antimicrobial agents, skin infections are increasingly difficult to treat. Infections caused by drug-resistant microorganisms are associated with high morbidity and mortality and consequently higher healthcare costs (Suaya *et al., 2014).* Therefore, there is a need to find/develop compounds with antimicrobial properties that are also cost effective. There is a growing interest in the use of silver nanoparticles (Ag NPs) for the treatment of SSTIs due to their improved properties (A Aljuffali *et al.,* 2015; Rai *et al.,* 2009).

Plants have been used as medicine by various cultures throughout history. They are an important source of phenolic compounds, mainly flavonoids, many of which have antimicrobial, anti-inflammatory and antioxidant properties that enhance the treatment of SSTIs (Mussin *et al.,* 2021).

The combination of traditional medicine with nanotechnology therefore opens the door to innovative strategies for the treatment of SSTIs and also contributes to the fight against the increase in antimicrobial resistance (Mussin *et al.,* 2021).

The present study illustrates the green synthesis of silver nanoparticles from citrus fruits extract. The synthesized nanoparticles were characterized by using different techniques. The antibacterial activities of Ag NPs were also studied to show their highly action on bacteria according to their particle size.

2. Material and Methods

This chapter details the research design used in this study such as synthesis and characterization of silver nanoparticles (Ag NPs), and it further describes methods that were chosen in the investigation of the antibacterial properties of these nanoparticles.

2.1. Materials

Citrus paradisi (Pink Grapefruit) were purchased from the local market, silver nitrate Ag NO_3 (Sigma Aldrich, Germany), (nutrient agar, MacConkey agar, blood agar, chocolate agar) (Oxoid Ltd., Basingstoke, UK), were used as a culture media.

Organisms used include: *Staphylococcus aureus*, *Escherichia coli*, *Klebsiella pneumoniae*, *Pseudomonas aeruginosa*. These were isolated soft tissue infecting patients at from Kasr Al-Aini Hospital, faculty of medicine, Cairo, Egypt.

2.2. Methods

2.2.1. Preparation of *Citrus paradisi* fruit extract

Fresh peels of *citrus paradisi* were collected, washed thoroughly with double distilled water and sliced into small pieces. *Citrus paradisi* peels (4 g) weighed and transfer into 250ml beaker containing 40ml double distilled water, mixed well and boiled for 2 min at hot plate. The extract obtained was filtered through Whatman No.1 filter paper and the filtrate was collected in 250ml Erlenmeyer flask. The method used to prepare *citrus paradisi* fruit extract followed (Kaviya *et al.,* 2011).

2.2.2. Synthesis of silver nanoparticles Ag NPs using citrus paradisi fruit extract:

Silver nanoparticles were synthesized via eco-friendly green method using *citrus paradisi* extract. Three flasks each containing 50 ml of silver nitrate (Sigma Aldrich, USA), aqueous solution (2 mM) were prepared. To study the effect of concentration of capping and reducing agent on the physical characteristics (and subsequently their antibacterial efficacy) of the prepared Ag NPs, different volumes (3,6 and 9 ml) of *citrus paradisi* fruit extract (act as capping and reducing agent) were added to each flask to prepare 1-Ag NPs, 2-Ag NPs, and 3-Ag NPs. Flasks were left at water bath (60°C) for 45 min, the color change from yellow to brown within 10 min indicating synthesis of Ag NPs and confirmation of reduction of Ag^{+} ion and formation of silver nanoparticles that monitored via UV spectrophotometer later (Kaviya *et al.,* 2011).

2.3. Characterization of Silver nanoparticles

The preliminary examination of silver nanoparticles solutions was carried out by visual observation of color change of mixture (brown color appeared).

Formation and stability of Ag NPs were determined by a UV-visible spectrophotometer, (Barloworld Scientific, Jenway UV-6420, Essex, UK). The average hydrodynamic diameter of the colloidal particles, and the polydispersity index (PdI) that described the width of particle size distribution were analyzed in a dynamic light scattering (DLS) instrument (Model Nano-ZS90, Malvern Instruments Ltd, Malvern, UK). Also, the measure of the surface charges (Fathy, 2020) of the hydrated particle size and zeta potential of prepared Ag NPs formulations were measured using a Zeta sizer instrument (Model Nano-ZS90, Malvern Instruments Ltd, Malvern, UK). The morphological characteristics and size of prepared nanoparticles were examined using TEM with JEOL, Japan (JEM-2100) electron microscope instrument, within accelerating voltage of 200kV after adding few drops of each Ag NPs aqueous solutions on the carbon grid coated copper. TEM grid samples were dried by lifting sample on a filter paper and left for 10 min before loading on a specimen holder (Fathy, 2020; Elamawi *et al.,* 2018).

2.4. Sample collection

2.4.1. Isolation

Bacteria were isolated from soft tissue infecting patients at Kasr Al-Aini Hospital, faculty of medicine, Cairo, Egypt, by using sterilized cotton swabs then I was submerged into saline solution (sodium chloride 0.9%). Subsequently, the swabs were carefully covered to prevent contamination, then transferred to laboratory within 2hr., isolates were sub-cultured on different culture media (nutrient agar, MacConkey agar, blood agar, chocolate agar) (Oxoid Ltd., Basingstoke, UK) under aerobic condition at 37°C overnight for obtain single colony. Nutrient agar medium composition (Atlas,2010); Yeast extract 2.0g/L, Peptone 5.0g/L, Sodium chloride 5.0g/L, Beef extract 1.0g/L, Agar 15g/L, Distilled water 1.0L, pH 7.4 ±0.2, Sterilized by autoclave at 121◦c for 15 min. MacConkey Agar (Atlas,2010); Pancreatic digest of Gelatin 17.0g/L, Agar 13.5g/L, Lactose 10.0g/L, NaCl 5.0g/L, Bile salts 1.5g/L, Pancreatic digest of casein1.5g/L, Peptic digest of animal tissue 1.5g/L, Neutral red 0.03g/L, Crystal violet 1.0mg/L, pH at 7.1±0.2. Blood Agar Base media (Atlas,2010); Agar 15.0g/L, Beef extract 10.0g/L, Peptone 10.0g/L, NaCl 5.0g/L, Sheep blood defibrinated 50.0ml, pH at 7.3±0.2. The contents were mixed thoroughly, heated with agitation. Boiled for 1 min to completely dissolve the powder and

autoclaved at 121˚C for 15 min. 50 ml of sterile sheep blood were added to the agar after cooling to 50˚C.

2.5. Purification

Single colony was streaked on agar surface of different diagnostic and selective media. Plates were incubated aerobically at (37˚ c for 24hr.). They were purified by subculturing several times to obtain pure cultures. Few biochemical tests were carried out to confirm these isolates before being used for the work. Growing colonies were purified and examined using biochemical properties and gram stain.

2.6. Identification

On solid media, a colony is theoretically derived from a single cell. If well separated from other colonies, a colony will have a characteristic shape (both in elevation and margin), size, color, and consistency. Observation is often made with the naked eye, but dissecting microscopes are also used (Breakwell *et al.,* 2007). The Isolates were identified by gram staining, colony morphology, and standard biochemical tests manually: catalase, coagulase, oxidase, Indole production, citrate utilization, urease, and triple sugar iron fermentation tests (Collee *et al.,* 2012)**.**

2.7. Morphological identification

Differential media (Klamm, 2019) Media supporting the growth of various types of microorganisms while providing an environment that makes it easy to distinguish various different forms by the addition of certain dyes or chemicals to the medium will cause microbes to produce characteristic changes or growth patterns that may be used for identification or differentiation.

Enriched media (Sonnenwirth, 1972): Addition of extra nutrients in the form of blood, serum, egg yolk etc. to basal medium makes them enriched media. It is usually in solid form. Enriched media are used to grow nutritionally exacting (fastidious) bacteria. Blood agar, chocolate agar, Loeffler's serum slope are few of the enriched media.

2.7.1. Microscopic examination

Gram stain (Harrigan and mcCance,1966)

Examine the bacteria in each circle and observe the size, shape (rod, spherical or curved), Gram staining (positive: purple; negative: pink), and arrangement (singly, in pairs, in chains, irregular clusters, or regular packets of four or eight). Compare the Gram-negative organism(s) with the Gram positive and note the difference in color. The Gram stain is especially useful as one of the first steps in the identification of a bacterial species, since it reveals both the morphology and the Gram reaction of the bacteria. In this exercise, both Gram-positive and Gram-negative rods and cocci of commonly encountered bacterial species will be stained. Examine the stained slides with low power objectives and finally use the oil immersion lens. On the basis of their reaction to the Gram stain, bacteria can be divided into two large groups: Gram positive and Gram negative. The different response of the two groups to the Gram stain is based on fundamental differences in cell wall structure and composition.

Reagents

Crystal violet solution		**Iodine solution**		**Decolorizing solution**		**Counter stain**	
Crystal violet	2.0g	Potassium iodide	2.0g	Acetone	50ml	Safranin	2.5g
Ethyl alcohol 95%	20ml	Iodine crystals	1.0g	Ethyl alcohol 95%	20ml	Ethyl alcohol 95%	100ml
Ammonium oxalate	0.8ml	Distilled water	100ml			Distilled water	100ml
Distilled water	100ml						

Steps: a heat fixed smear from an 18-24hr bacterial culture was prepared on a clean slide. Place the slide on a staining rack, then Add 2-3 drops of crystal violet stain directly on the smear. Stain for one minute. Rinse the slide by washing the stain off with water. Add 2-3 drops of Gram's iodine solution. Let the slide for one minute. Decolorize the stain by the decolorizing solution, until the stain is removed not more than 20 sec. Finally, add 2-3 drops of safranin stain and let stain for 30 seconds. Then rinse the slide with water Let the slide air-dry, or blot it dry with blotting paper. The slide should be completely dry before adding oil for microscopic examination.

2.8. Biochemical identification

Identification was carried out by traditional biochemical tests according to (Collee *et al.,* 2012). isolates also identified automatically by using the VITEK 2 – compact 15 computer automatic bacteria identification system (BIOMÉRIUX, USA) (Liao *et al.,* 2019).

Catalase test (Baron,1996) activity was determined by bubble production in H_2O_2 solution. Coagulase test (Baron,1996) was determined by Clumping of cocci within 5-10 sec. Oxidase test (Kovács, 1956) activity was determined by oxidase discs formation of blue purple color within 10-15 seconds. Indole production test (Bergey, 1994) activity was determined by Indole gas combines with the reagent, forming red ros indole dye. Citric acid utilization (Winn *et al.,* 2006), Urease test (Harley, 2005), and Triple sugar iron fermentation test (H_2S production) (Hemraj, 2013) were also determined.

Pure and identified bacterial isolates were applied for *Klebsiella pneumoniae*, *Staphylococcus aureus*, *E. coli and Pseudomonas aeruginosa*, and then checked according to (Breakwell *et al.,* 2007; Collee *et al.,* 2012).

These identified cultures were transferred to nutrient agar slants for preservation and then store in the refrigerator at 4°C (Omar &Jabber,2017).

2.9. Antibacterial activity of silver nanoparticles against soft tissue-infecting bacteria experiments

2.9.1. Agar-well diffusion method:

Ag NPs were examined for their effect on Gram-negative and Gram-positive pathogenic microbes using well diffusion. In the well diffusion method, Pure cultures of micro-organisms were sub-cultured on Nutrient agar, then make bacterial suspension was prepared and spectrophotometrically adjusted to match the turbidity of 0.5 McFarland in (OD_{625}) (Wiegand *et al.,* 2008; Jonasson *et al.,* 2020). Subsequently, fresh culture of each test organism was spread on Mueller-Hinton agar plates. To evaluate the antibacterial activity of nanoparticles, three adequately wells of 6 mm diameter each were made at the culture agar surface using a sterile cork-borer. 160μL of each sample (1-AgNPs, 2-AgNPs, and 3-AgNPs) was poured onto wells, using a micropipette. The plates were incubated for 24h at 37∘C; and zones of inhibitions were measured in diameter. In this experiment, Ag NPs solutions (24 µg ml^{-1}) was compared with plant extract (negative control) and LEV antibiotic (positive control) against pathogenic bacteria. The zone of inhibition was measured after 24 h of incubation. All experiments were performed in triplicates for confirmation the results (Mohammed, 2015).

2.9.2. Kirby-Bauer Disc Diffusion method (Heatley, 1944; CLSI 2012)

Is the official method used in many clinical microbiology laboratories for routine antimicrobial susceptibility testing. Nowadays, there are many accepted and approved standards published by clinical laboratory standard institute CLSI for bacteria testing (CLSI, 2012). This test was performed as described previously using Mueller Hinton agar MHA, make bacterial suspension was prepared and spectrophotometrically adjusted to match the turbidity of 0.5 McFarland in (OD_{625}) (Wiegand *et al.,* 2008; Jonasson *et al.,* 2020). Subsequently, fresh culture of each test organism was spread on Mueller-Hinton agar plates. Then, sterilized filter paper discs (about 6 mm diameter), impregnated with different samples of Ag NPs (1-AgNPs, 2-AgNPs, and 3-AgNPs), are placed on the agar surface. Filter paper discs loaded with 15µl fruit peel extract used as a negative control (Gopinath *et al.,* 2012). The zone of inhibition was measured after 24 h of incubation. All experiments were performed in triplicates for confirmation the results (Mohammed, 2015).

2.9.3. Microdilution Method: The minimum inhibitory concentration (MIC) and Minimum bactericidal concentration (MBC) (Cockerill *et al.,* 2010)

MIC and MBC of the Ag NPs was assessed by the microdilution method according to the guidelines presented by the CLSI (Cockerill *et al.,* 2010). Bacterial strains were cultured in Mueller Hinton Broth (MHB), prepared and was spectrophotometrically adjusted to match the turbidity of 0.5 McFarland in (OD_{625}) (JENWAY 6300 spectrophotometer, JENWAY Ltd., Essex, England) ((Wiegand *et al.,* 2008; Jonasson *et al.,* 2020). serial dilutions from each Ag NPs concentration were prepared in a 96-well microplate (Abbaszadegan *et al.,* 2015). 100µL of the 0.5 McFarland of each bacterial suspension was dispensed into a 96-well ELISA (enzyme-linked immunosorbent assay) plate. *P. aeruginosa, E. coli, Staph. aureus MRSA* and *K. pneumoniae* were then exposed to different samples of Ag NPs (Abbaszadegan *et al.,* 2015). Then the 3 samples of Ag NPs that we have, serial dilution from 24 to 0.0468 µg/ml was prepared by using deionized distilled sterilized H_2O. 100µl from each dilution and concentration of Ag NPs was added to wells, the final volume of 200 µl. Two wells 11 &12 were considered as negative and positive control. Nutrient broth media used as a negative control and 0.5 McFarland bacterial suspension used as a positive control. The ELISA plate was incubated at 37°C for 24 hr. (Fozouni *et al.,* 2019). The optical density of wells was obtained by an ELISA reader apparatus (Awareness Technologies Inc. Stat Fax 2100 Microplate reader) at a wavelength 590 nm. MBC test was performed by plating the suspension from each well of ELISA plate into Muller Hinton agar MHA plate. The plates were incubated at 37°C for 24 hr. The lowest concentration with no visible growth on MHA plate was taken as MBC value (Loo *et al.,* 2018).

2.9.4. Antibiotic-susceptibility test

Test performed using Kirby-Bauer Disc Diffusion method on Muller-Hinton agar (MHA) (Oxoid Ltd., Basingstoke, UK) according to Clinical and Laboratory Standard Institute (CLSI) guidelines. The test is performed by applying a bacterial inoculum the turbidity of 0.5 McFarland to the surface of Mueller-Hinton agar plate. Up to 28 commercially prepared, fixed concentration, paper antibiotic disks are placed on the inoculated agar surface. Plates are incubated for 16–24 h at 35°C prior to determination of results. The following antibiotics were tested (Hi Media Laboratories Pvt. Ltd., Thane, (West) 400604, India): Polimixin B (PB) (300unit), Ciprofloxacin CIP (5µg), Tigecyclin TGC (15µg), Aztreonam AT(30µg), Cefepime FEP (30µg), Cefoxitin CX (30µg), Ceftriaxone CTR (30µg), Amoxicillin/Clavulanic acid AMC (30µg), Ceftazidime CAZ (30µg), Piperacillin/Tazobactam PIT (100/10µg), Imipenem IPM (10µg), Meropenem MRP (10µg), Amikacin AK (30µg), Co-Trimoxazole (Sulpha/Trimethoprim) COT (25µg), Ampicillin AMP (10µg), Gentamicin GEN (10µg), Ofloxacin OF (5µg), Levofloxacin LEV (5µg), Doxycycline Hydrochloride DO (30µg), Erythromycin E (15µg), Clindamycin CD (2µg), Vancomycin VA (30µg), Ampicillin/Sulbactam A/S (10/10 µg), Azithromycin AZM (15µg), Linezolid LZ (30µg), Cefaclor CF (30µg), Teicoplanin TEC (30µg), Cefuroxime CXM (30µg) (Ahmed *et al.,* 2020).

2.9.5. The transmission microscopic study of different bacterial isolates treated with silver nanoparticles Ag NPs

To analyze the action of synthesized silver nanoparticles Ag NPs on bacterial isolates, the isolates were inoculated in Mueller Hinton agar and incubated at 37°C for 24h., then make 0.5 McFarland by taking a single colony and put it in Mueller Hinton broth MHB and measure the absorption at a wavelength of 625 nm should be in the range from 0.08 to 0.13 (Wiegand *et al.,* 2008; Jonasson *et al.,* 2020).Bacterial isolates suspension at mid log phase subjected to the sub-Mic of the different samples of Ag NPs (1-Ag NPs, 2-Ag NPs and 3-Ag NPs) at 37°C for 6 hr., according to the origin and susceptibility profile of each isolate, using clinically relevant concentrations (Adamis *et al.,* 2004, Ahsman *et al.,* 2010). In all the processes, a control for the isolates was included under the same conditions and at the same dilutions, without the presence of the Ag NPs. The interaction between nanoparticles and bacteria was observed by TEM. Briefly, the suspension of the materials was sonicated for 20 min on ultra-sonicator (Crest Ultrasonics Corp., New Jersey, USA). Then the suspension were fixed using 2.0% glutaraldehyde (Sigma-Aldrich). Post fixation was performed using 1% osmium tetroxide (Electron Microscopy Science) followed by dehydration using ethanol (Sigma-Aldrich). After dehydration, few drops were loaded on carbon coated copper grid, and left to dry. The grid loaded with the sample was examined by HR-TEM (JEOL, JEM-2100, Tokyo, Japan), operated at 160kv.

I compare two bacteria at mid log phase (*Staphylococcus aureus* and *Pseudomonas aeruginosa*) with two samples at the supra-MIC of Ag NPs (2-AgNPs and 3-AgNPs) to visualize the cell membrane of *S. aureus* and *P. aeruginosa* after exposure to Ag NPs and to study morphological changes occurring on the bacterial surface.

2.10. Statistical analysis

Data are presented as means ± SD of at least three independent experiments. Comparisons are made by the student's t-test or by ANOVA when appropriate. Differences are considered statistically significant at $p < 0.05$. Statistical analysis was carried out estimated by Minitab software, (version 2021).

2.11. Verification experiments the predicted optimum levels

For the independent variables were carried out and compared with the basal conditions and the averages of inhibition zones were calculated. This experiment was performed in triplicate. Silver nanoparticles and their antibiotic efficacy the antimicrobial activity of the biosynthesized Ag NPs was examined against bacterial pathogens.

3. Results and Discussion

3.1. Characterization of synthesizes silver nanoparticles Ag NPs

The addition of *citrus paradisi* fruit extract (as a capping agent for silver nanoparticles) to $AgNO_3$ solution the color was change from colorless to yellowish brown within 10 min (Fig. 1). This indicated formation of silver nanoparticles. brown color in the synthesis medium happened due to the reduction of silver ions to Ag NPs. This correlated very well with the known phenomenon of surface plasmon resonance (SPR) property of Ag NPs. Fig. 2 shows UV-is spectra recorded for nanoparticles formulations (1-Ag NPs, 2-Ag NPs, and 3-Ag NPs) showed characteristic surface plasmon resonance band in the range of 200–205 nm. UV-vis spectra show an optical absorption narrow band peak at 205 nm, 205, and 205 nm. Interestingly, 1-SNPs display broad band at 260nm that may be due to non-homogenous size distribution of the prepared colloid. The size distribution of the prepared silver nano-formulation was determined via DLS (Fig. 3), For 1-Ag NPs sample, the average hydrodynamic size was 180.8 nm with PDI of 0.396, for 2-Ag NPs sample, the average hydrodynamic size was 118.5 nm with PDI 0.308, and for sample 3-Ag NPs the average hydrodynamic size was 91.59 with PDI 0.259. sample 3-Ag NPs has the smallest PDI and average hydrodynamic size indicating that it has a monodispersed nature compared to the other samples. Zeta potential measurements for the prepared nano-formulations (1-Ag NPs, 2-Ag NPs, 3-Ag NPs) showed that all nano-formulations have negatively surface charge with values -21.3±2.2mV, -26.9± 3.4mV, and -28.9±2.5mV for 1-Ag NPs, 2-Ag NPs, and 3-Ag NPs, respectively (Fig. 4). Based on the results, 2-Ag NPs and 3-Ag NPs have higher negatively surface charge than 1-Ag NPs. The size and morphology of Ag NPs were confirmed via transmission electron microscopy TEM According to transmission Electron Microscopy (TEM) images (Fig. 5), the nano-formulations were synthesized with various sizes (4.9-56.3nm, 6.87-26.11nm, and 3.16-13.45nm for 1-Ag NPs, 2-Ag NPs, and 3-Ag NPs, respectively) and with mostly spherical morphology (Figure 5a-c). Interestingly, 3-Ag NPs (Figure 5 C) reveals that the particles are well dispersed, non-aggregated and spherical in shape, while some particles (Figure 5 A and B) are found to be aggregated and having anisotropic structures of irregular shapes. The prepared nanoparticles were surrounded with a faint thin layer which might be capping agent of fruit extract.

From the above results, it was found that the Ag NPs that green synthesized from fruit extract were a good candidate to continue the next experiments for some applications of Ag NPs such as antimicrobial activities against the identified organisms.

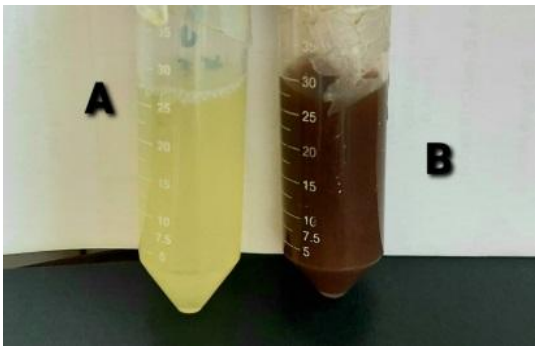

Fig. 1: Show change in color of fruit extract from yellow to yellowish brown (A) *citrus paradisi* fruit extract, (B)biosynthesized silver nanoparticles at 60°C.

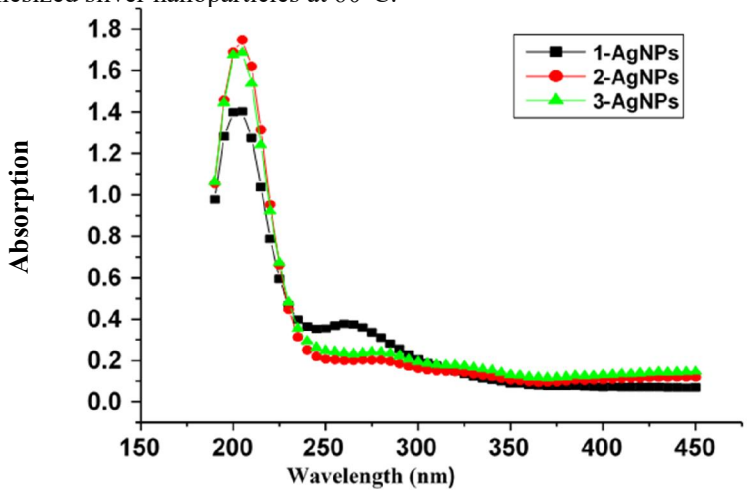

Fig. 2: UV–vis absorption spectrum of silver nanoparticles synthesized at 60 °C at different volumes of *citrus paradisi* fruit extract, (A) Ag NPs with 3 ml *citrus paradisi* fruit extract (1-Ag NPs) (B) Ag NPs with 6 ml *citrus paradisi* fruit extract (2-Ag NPs) (C) Ag NPs with 9 ml *citrus paradisi* fruit extract (3-Ag NPs).

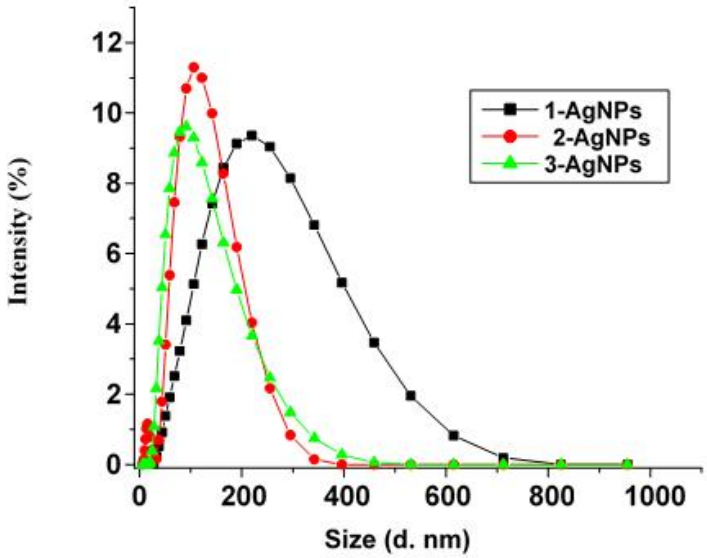

Fig. 3: Dynamic light scattering analysis of Ag NPs samples distribution concerning size and intensity**.**

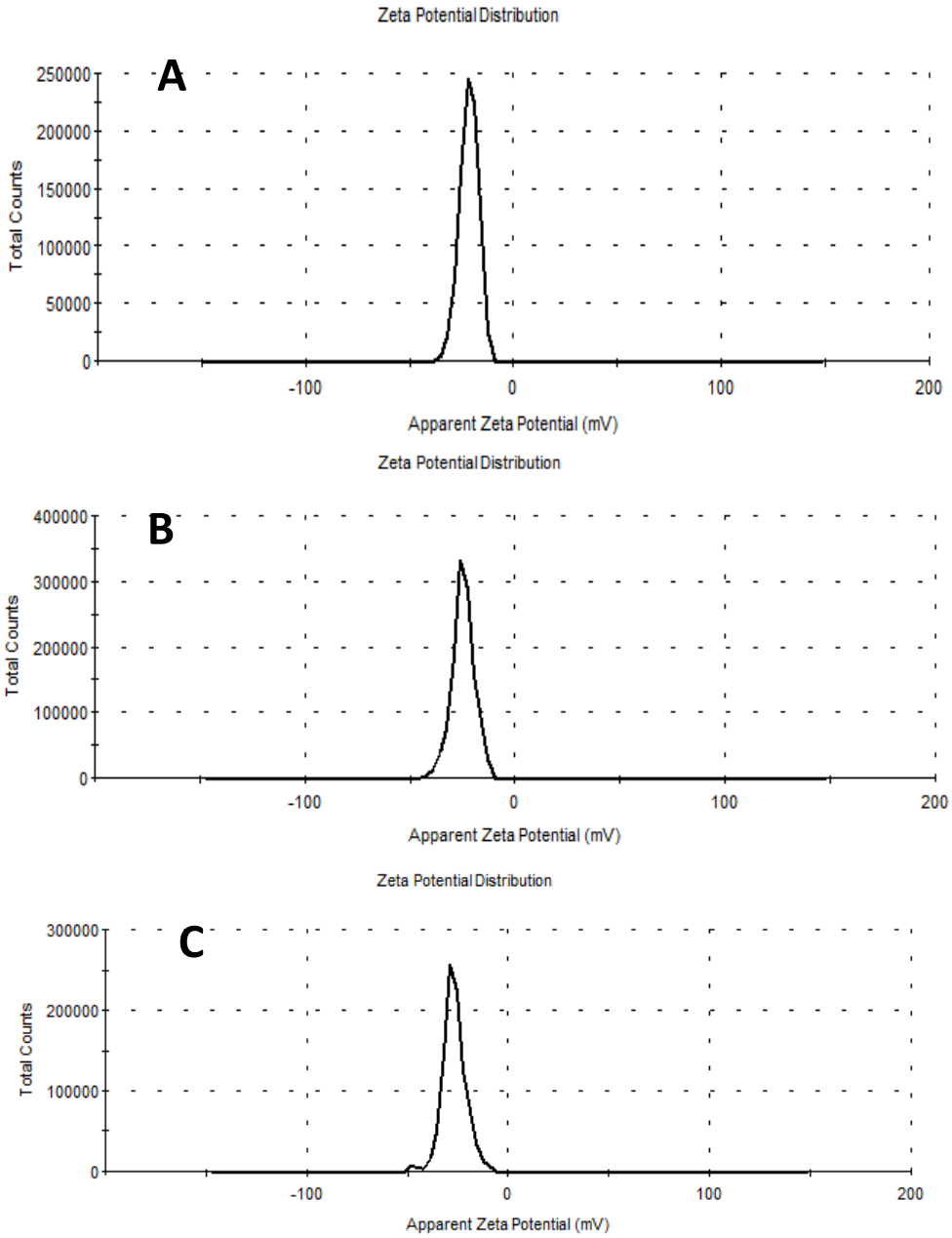

Fig. 4: Zeta potential distribution (A) Zeta potential distribution for 1-Ag NPs (B) Zeta potential distribution for 2-Ag NPs (C) Zeta potential distribution for 3-Ag NPs**.**

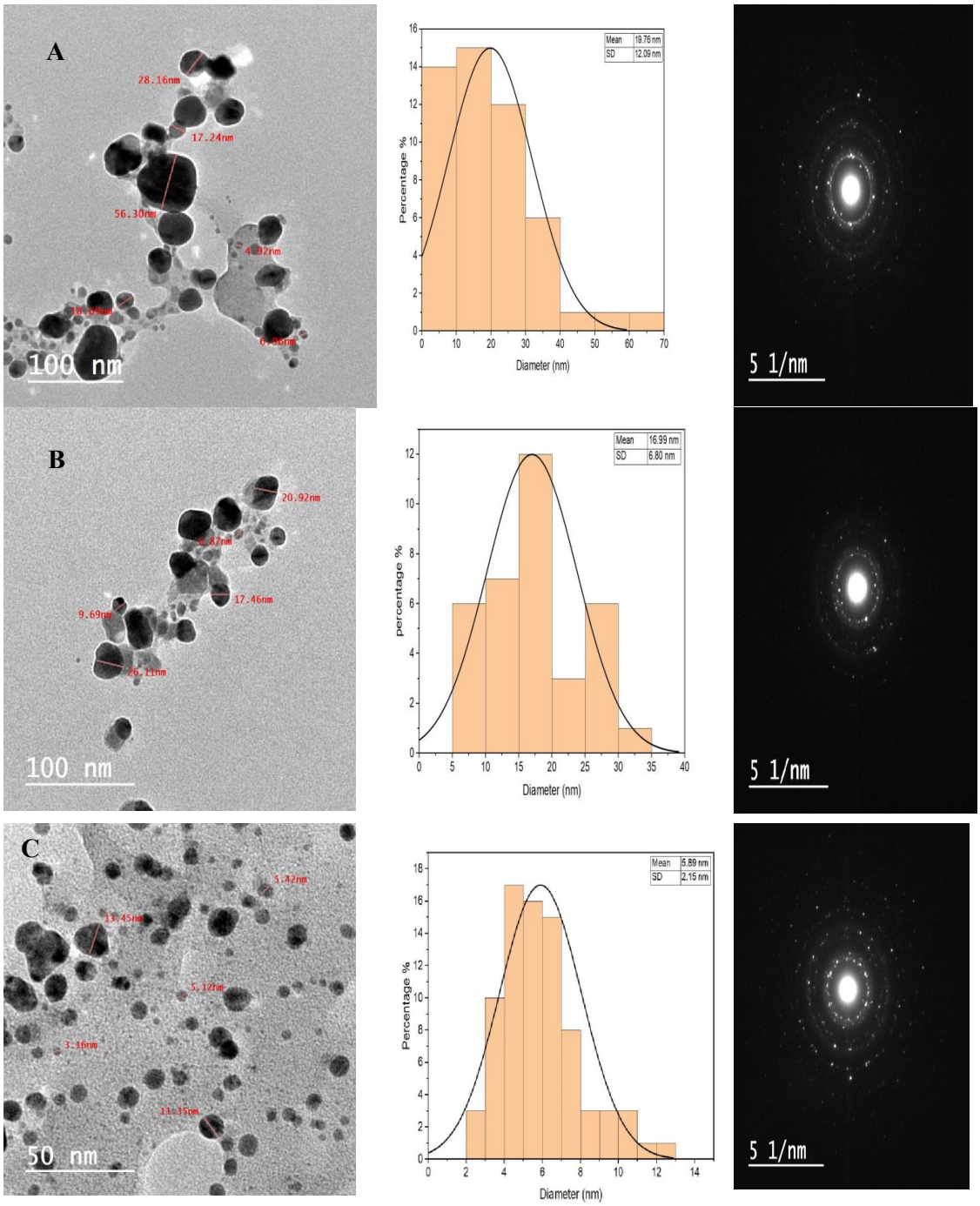

Fig. 5: TEM micrograph recorded on a drop-coated film with *Citrus Paradisi* fruit extract and Ag NPs aqueous suspension. A) Sample 1-Ag NPs with electron diffraction and size distribution B) Sample 2-Ag NPs with electron diffraction and size distribution C) Sample 3-Ag NPs with electron diffraction and size distribution**.**

3.2. Morphological, cultural, Biochemical and physiological tests for Identification of bacterial isolates

The morphological observations in Gram's staining revealed presence of Gram positive and gram-negative bacteria, in microscopic analysis, some bacteria were of round shape and some were rod shape (Data no shown). The gram-negative property was further confirmed by growth on MacConkey's agar and other medium such as Eosin methylene blue (EMB) agar and Cetrimide agar, but gram-positive

property was confirmed by growth of bacteria on Blood agar, Mannitol salt agar MSA medium, and Baird-Parker agar. The isolates are definitively identified in Table (1) which was further confirmed by culturing the isolates on different media and tested biochemically to screen the presence of some enzymes like oxidase, catalase, coagulase and so on (Table 2). The isolates also identified and confirmed automatically via Vitek-2 compact instrument (Tables 3,4,5 and 6). The isolates were correctly identified as *E. coli, Klebsiella pneumoniae*, *Staph. aureus,* and *Pseudomonas aeruginosa*, respectively.

Table 1: Growth on various media and bacterial apparent.

Bacteria **Cultural Media**	***E. coli***	***K. pneumoniae***	***S. aureus***	***P. aeruginosa***
Blood agar media	Greyish white moist colonies	white mucoid colonies	Golden colonies with B-hemolysis	Smooth, mucoid Greyish white
MacConkey agar	Pink colonies and lactose fermenting	Pink colonies and non-lactose fermenting	No growth	Colonies produce green pigment
Mannitol salt agar	-	-	Small colonies surrounded by yellow zone	-
Baird-parker medium	-	-	Black colonies	-
Eosin methylene blue medium	Dark center and green metallic sheen	-	-	-
Cetrimide agar	-	-	-	Enhance fluorescence and pyocyanin pigment (bright green color)

Table 2: Biochemical tests. (+): Positive results. (-): Negative results.

Bacteria **Test**	***E. coli***	***K. pneumoniae***	***S. aureus***	***P. aeruginosa***
Catalase test	**(+)**	**(+)**	**(+)**	**(+)**
Coagulase test	**(-)**	**(-)**	**(+)**	**(-)**
Oxidase test	**(-)**	**(-)**	**(-)**	**(+)**
Indole production test	**(+)**	**(-)**	**(-)**	**(-)**
Citric acid utilization test (Simmon citrate)	**(-)**	**(+)**	**(+)**	**(+)**
Urease test	**(-)**	**(+)**	**(+)**	**(-)**
Triple sugar iron test	Acid/Acid Yellow/Yellow	Acid/Acid Yellow/Yellow	Acid/Acid Yellow/Yellow	Alkali/alkali Red/Red

Table 3: Automated biochemical identification of *E.coli* bacteria by Vitek 2-compact system.

bioMérieux customer: Microbiology Chart Report Printed October 12, 2022 11:28:51 AM CDT

Patient Name: Dr, Hadeer Patient ID: 12010202201
Location: Physician:
Lab ID: 111 Isolate Number: 1

Organism Quantity:
Selected Organism: ***Escherichia coli***
Source: **Collected:**

Comments:	

Identification Information	**Analysis Time:** 4.83 hours	**Status:** Final
Selected Organism	90% Probability ***Escherichia coli*** **Bionumber:** 2415611550524610	
ID Analysis Messages		

Biochemical Details

2	APPA	–	3	ADO	+	4	PyrA	-	5	lARL	-	7	dCEL	-	9	BGAL	+
10	H2S	+	11	BNAG	–	12	AGLTp	_	13	dGLU	+	14	GGT	_	15	OFF	+
17	BGLU	_	18	dMAL	+	19	dMAN	+	20	dMNE	+	21	BXYL	_	22	BAlap	_
23	ProA	+	26	LIP	_	27	PLE	_	29	TyrA	+	31	URE	_	32	dSOR	+
33	SAC	+	34	dTAG	_	35	dTRE	+	36	CIT	_	37	MNT	_	39	5KG	_
40	ILATk	+	41	AGLU	_	42	SUCT	+	43	NAGA	_	44	AGAL	+	45	PHOS	_
46	GlyA	_	47	ODC	_	48	LDC	_	53	IHISa	_	56	CMT	+	57	BGUR	+
58	O129R	+	59	GGAA	_	61	IMLTa	_	62	ELLM	_	64	ILATa	_			

Table 4: Automated biochemical identification of *Klebsiella pneumoniae* bacteria by Vitek 2-compact system.

bioMérieux customer: Microbiology Chart Report Printed October 12, 2022 11:27:58 AM CDT

Patient Name: Dr, Hadeer Patient ID: 12010202202
Location: Physician:
Lab ID: 222 Isolate Number: 1

Organism Quantity:
Selected Organism: ***Klebsiella pneumoniae*** **spp** ***pneumoniae***
Source: **Collected:**

Comments:	

Identification Information	**Analysis Time:** 3.83 hours	**Status:** Final
Selected Organism	96% Probability ***Klebsiella pneumoniae*** **spp** ***pneumoniae*** **Bionumber:** 6607734753564410	
ID Analysis Messages		

Biochemical Details

2	APPA	–	3	ADO	+	4	PyrA	+	5	lARL	-	7	dCEL	+	9	BGAL	+
10	H2S	–	11	BNAG	–	12	AGLTp	_	13	dGLU	+	14	GGT	+	15	OFF	+
17	BGLU	+	18	dMAL	+	19	dMAN	+	20	dMNE	+	21	BXYL	+	22	BAlap	_
23	ProA	_	26	LIP	_	27	PLE	+	29	TyrA	+	31	URE	+	32	dSOR	+
33	SAC	+	34	dTAG	_	35	dTRE	+	36	CIT	+	37	MNT	+	39	5KG	_
40	ILATk	+	41	AGLU	_	42	SUCT	+	43	NAGA	_	44	AGAL	+	45	PHOS	+
46	GlyA	_	47	ODC	_	48	LDC	+	53	IHISa	_	56	CMT	_	57	BGUR	+
58	O129R	+	59	GGAA	_	61	IMLTa	_	62	ELLM	_	64	ILATa	_			

Table 5: Automated biochemical identification of *Staphylococcus aureus* bacteria by Vitek 2-compact system.

bioMérieux customer: Microbiology Chart Report Printed October 13, 2022 9:39:00 AM CDT

Patient Name: Dr, Hadeer Patient ID: 12010202201
Location: Physician:
Lab ID: 3333 Isolate Number: 1

Organism Quantity:
Selected Organism: ***Staphylococcus aureus***
Source: **Collected:**

Comments:	

Identification Information	**Analysis Time:** 8.00 hours	**Status:** Final
Selected Organism	87% Probability ***Staphylococcus aureus***
	Bionumber: **0700020777732 71**
ID Analysis Messages	

Biochemical Details

2	AMY	–	4	PIPLC	–	5	dXYL	–	8	ADHI	+	9	BGAL	+	11	AGLU	+
13	APPA	–	14	CDEX	–	15	AspA	_	16	BGAR	_	17	AMAN	_	19	PHOS	–
20	LeuA	–	23	ProA	–	24	BGURr	–	25	AGAL	_	26	PyrA	+	27	BGUR	_
28	AlaA	_	29	TyrA	_	30	dSOR	–	31	URE	+	32	POLYB	+	37	dGAL	+
38	dRIB	+	39	ILATK	+	42	LAC	+	44	NAG	+	45	dMAL	+	46	BACI	+
47	NOVO	+	50	NC6.5	+	52	dMAN	+	53	dMNE	+	54	MBdG	+	56	PUL	–
57	dRAF	–	58	O129R	+	59	SAL	_	60	SAC	+	62	dTRE	+	63	ADH2s	+
64	OPTO	+															

Table 6: Automated biochemical identification of *Pseudomonas aeruginosa* bacteria by Vitek 2-compact system.

bioMérieux customer: Microbiology Chart Report Printed October 31, 2021 10:09:18 AM CDT

Patient Name: P.seudo, Abeer Patient ID: 2610202101
Location: Physician:
Lab ID: abeerps Isolate Number: 1

Organism Quantity:
Selected Organism: ***Pseudomonas aeruginosa***
Source: **Collected:**

Comments:	

Identification Information	**Analysis Time:** 4.83 hours	**Status:** Final
Selected Organism	99% Probability ***Pseudomonas aeruginosa***
	Bionumber: 0043053103500040
ID Analysis Messages	

Biochemical Details

2	APPA	–	3	ADO	–	4	PyrA	–	5	IARL	–	7	dCEL	–	9	BGAL	–
10	H2S	–	11	BNAG	–	12	AGLTp	+	13	dGLU	+	14	GGT	+	15	OFF	–
17	BGLU	–	18	dMAL	–	19	dMAN	–	20	dMNE	+	21	BXYL	–	22	BAlap	+
23	ProA	+	26	LIP	+	27	PLE	–	29	TyrA	+	31	URE	–	32	dSOR	–
33	SAC	–	34	dTAG	–	35	dTRE	–	36	CIT	+	37	MNT	+	39	5KG	–
40	ILATK	+	41	AGLU	–	42	SUCT	+	43	NAGA	–	44	AGAL	–	45	PHOS	–
46	GlyA	–	47	ODC	–	48	LDC	–	53	IHISa	–	56	CMT	–	57	BGUR	–
58	O129R	–	59	GGAA	–	61	IMLTa	+	62	ELLM	–	64	ILATa	–			

3.3. Antibacterial activity of Ag NPs:

3.3.1. Well diffusion method:

We explored the antibacterial activity of produced Ag NPs against the isolated bacteria, to test the effectiveness and efficiency of nanoparticles against pathogens. The results showed that the green synthesized Ag NPs has a strong inhibitory effect on the growth of pathogenic microbes compared to the control (plant extract) with no inhibition zone occur (Fig 7E-H). The effect of biosynthesized silver nanoparticles samples was the highest inhibition in growth of *Klebsiella pneumoniae* with an inhibition zone reached to of 25.4±2.61 mm at sample 1-Ag NPs, and *Staph. Aureus* with an inhibition zone reached to of 25.1±1.73 mm also at sample 1-Ag NPs (Table 7), (Fig.6&7). The effect of biosynthesized silver nanoparticles samples was the lowest inhibition in growth of *Pseudomonas aeruginosa* with an inhibition zone ranges from 14±3.42mm, 14.1±2.43mm and 14,4±2.23mm at the samples 1-Ag NPs, 2-Ag NPs and 3-Ag NPs, respectively. Also, the 1-Ag NPs sample inhibit other bacteria, such as *E. coli* with an inhibition reached to of 25±2.13mm. The sample 2-Ag NPs also inhibit the bacteria *E. coli, Staph. aureus* and *Klebsiella pneumoniae* with an inhibition zone reached to of 24.7±1.75mm, 24.3±1.66mm, and 24.2±1.8mm, respectively. The sample 3-Ag NPs inhibit the bacteria *E. coli, Staph. aureus* and *Klebsiella pneumoniae* with an inhibition zone reached to of 23.83±2.59mm, 23.58±2.39mm, and 24.58±3.96mm, respectively. All these results are shown in (table 7) and (figure6& 7A-D). The results of ANOVA showed a significant bactericidal effect between the concentration of Ag NPs (24 µg/ml) and the diameter of the inhibition zone of the bacteria *P. aeruginosa, K. pneumoniae*, *Staph. aureus* and *E. coli* ($P < 0.05$ using t-test) (Table 8).

Table 7: Antimicrobial Activity test by well diffusion method for different samples Synthesized silver nanoparticles.

Samples Tested Bacteria	Inhibition Zone(mm)			Controls	
	1-AgNPs	2-AgNPs	3-AgNPs	-ve control	+ve control
E. coli	25±2.13	24.7±1.75	23.83±2.59	-	13
K. pneumoniae	25.42±2.61	24.2±1.8	24.58±3.96	-	13
P. aeruginosa	14.4±2.23	14.1±2.43	14.08±3.42	-	43
Staph. aureus	25.1±1.73	24.3±1.66	23.58±2.39	-	19

Table 8: P-value result of well diffusion method.

Sample	T-Value	P-Value
1-AgNps(3ml)	8.33	0.004
2-AgNps(6ml)	8.45	0.003
3-AgNps(9ml)	8.59	0.003

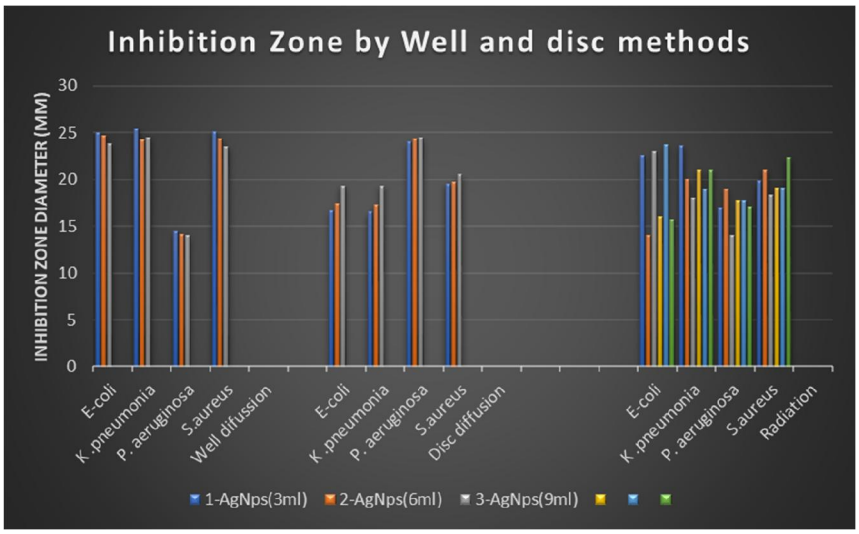

Fig. 6: Antimicrobial Activity test under well, Disc diffusion methods for different samples of Synthesized silver nanoparticles (Data are presented as mean ± SD, n = 4).

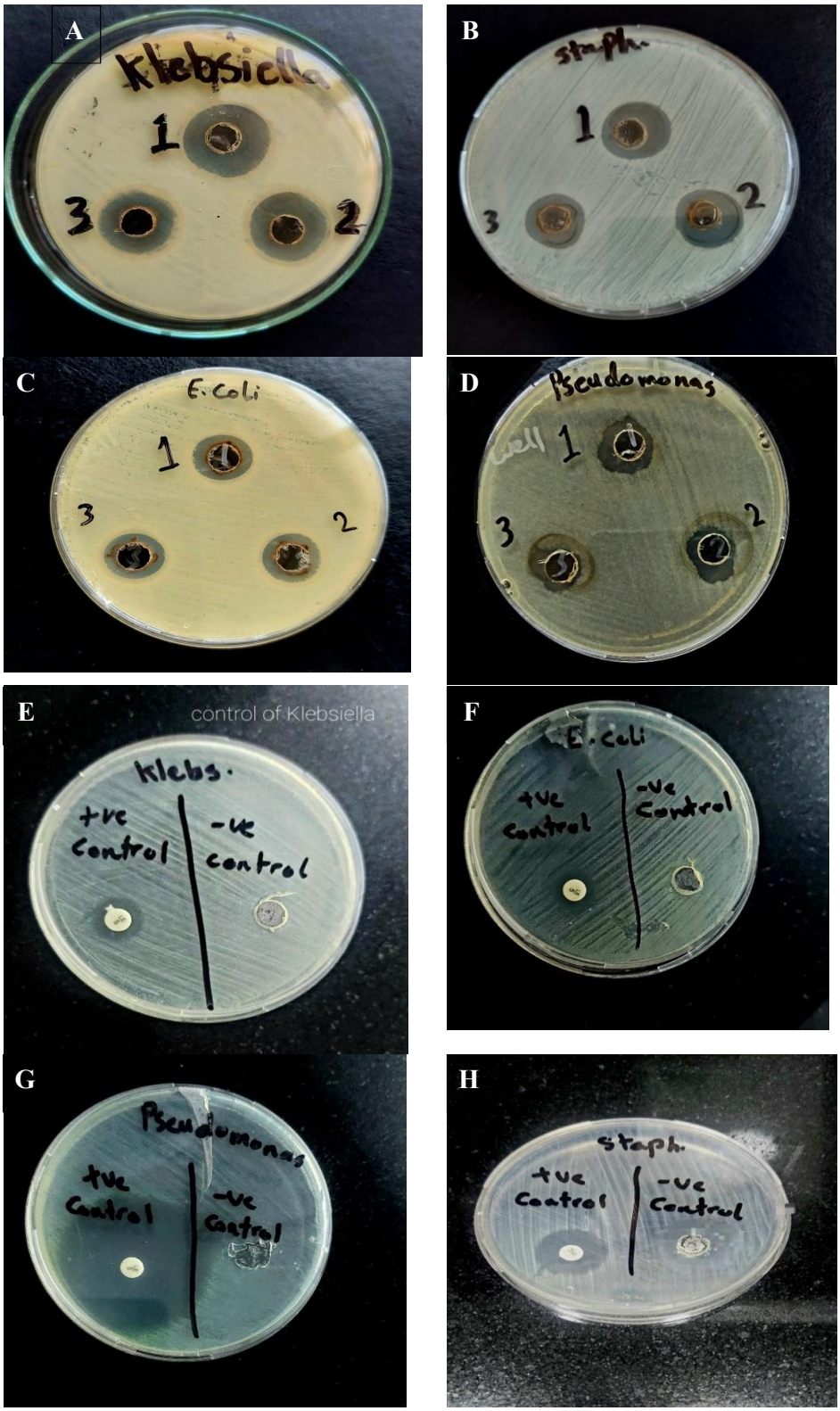

Fig. 7: Zone of inhibition of Ag NPs samples by well diffusion method against (A) *Klebsiella pneumoniae*, (B) *Staphylococcus aureus,* (C) *E. coli,* (D) *Pseudomonas aeruginosa.* (E) -ve and +ve control for *Klebsiella pneumoniae*, (F) -ve and +ve control for *E. coli*, (G) -ve and +ve control for *Pseudomonas aeruginosa*, (H) -ve and +ve control for *Staphylococcus aureus*. 1= 1-Ag NPs, 2= 2-Ag NPs, 3= 3-Ag NPs.

3.3.2. Kirby-Bauer Disc Diffusion method:

The diameter of inhibition zone in millimeter is shown in (Table 10) and (Fig. 8). The Ag NPs exhibited more activity than leaves extract (taken as negative control) (Fig. 6&Table10). The effect of biosynthesized silver nanoparticles samples was the highest inhibition in growth of *Pseudomonas aeruginosa* by the zone 24.4±1.51mm and 24.3±1.50mm at samples 3-Ag NPs and 2-Ag NPs respectively. The effect of biosynthesized silver nanoparticles samples was the lowest inhibition in growth of *Klebsiella pneumoniae* by zone 16.5±0.52mm. *Pseudomonas aeruginosa* bacteria have the highest zones diameter at the three samples of Ag NPs in contrast to the other bacteria with an inhibition zone 24±2.76mm, 24.3±1.50mm and 24.4±1.51mm at samples 1-Ag NPs, 2-Ag NPs and 3-Ag NPs respectively. Ag NPs three samples have a moderate effect at *Staphylococcus aureus* by the zone of inhibition values 19.5±3.53mm, 19.75±0.87mm and 20.5±2.32mm to 1-Ag NPs, 2-Ag NPs and 3-Ag NPs respectively given at (table 10). All tested Gram-negative and Gram-positive bacteria were highly susceptible to Ag NPs at 24 µg/ml concentration within 24 h of incubation.

The results of ANOVA showed a significant bactericidal effect between the concentration of Ag NPs (24 µg/ml) and the diameter of the inhibition zone of the bacteria *P. aeruginosa, K. pneumoniae*, *Staph. aureus* and *E. coli* ($P < 0.05$ using t-test) (Table 11).

Table 9: Antimicrobial Activity test by disc diffusion method for different samples Synthesized silver nanoparticles.

Samples / Tested bacteria	Inhibition Zone(mm)			Controls	
	1-AgNPs	2-AgNPs	3-AgNPs	-ve control	+ve control
E. coli	16.7±0.5	17.4±0.51	19.3±0.49	-	13
K. pneumonia	16.5±0.52	17.3±0.49	19.3±0.78	-	13
P. aeruginosa	24±2.76	24.3±1.50	24.4±1.51	-	43
S. aureus	19.5±3.53	19.75±0.87	20.5±2.32	-	19

Table 10: P-value results for disc diffusion method.

Sample	T-Value	P-Value
1-AgNPs(3ml)	10.94	0.002
2-AgNPs(6ml)	11.99	0.001
3-AgNPs(9ml)	17.23	0.000

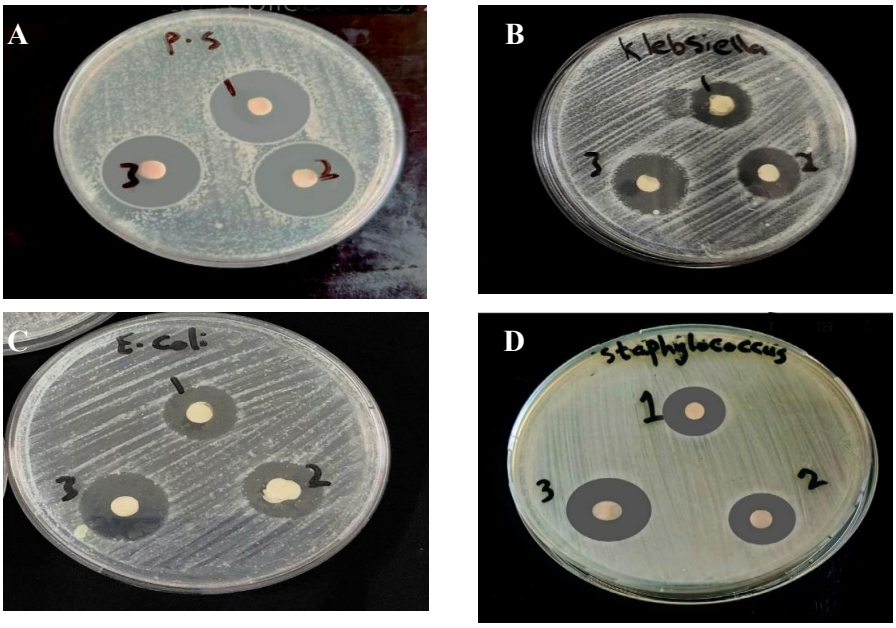

Fig. 8: Zone of inhibition of Ag NPs samples by disc diffusion method against (A) *Pseudomonas aeruginosa*, (B) *Klebsiella pneumoniae,* (C) *E. coli,* (D) *Staphylococcus aureus*. 1= 1-Ag NPs, 2= 2-Ag NPs, 3= 3-Ag NPs.

3.3.3. Microdilution Method: The minimum inhibitory concentration (MIC) and Minimum bactericidal concentration (MBC).

Ag NPs that synthesized from *Citrus paradisi* extract show antimicrobial activity against all tested bacterial isolates. Ag NPs 3 samples inhibited the growth of *E. coli* at the MIC of 0.094 µg/ml and the MBC of 0.188 µg/ml (Table 12). Also, Ag NPs 3 samples inhibited the growth of *Klebsiella pneumoniae* at the MIC of 0.047 µg/ml and the MBC of 0.094 µg/ml (Table 15). Both, samples 2-SNPs and 3-SNPs inhibited the growth of *Staph. aureus* at the MIC of 0.094 µg/ml and the MBC of 0.188 µg/ml. While sample 1-SNPs inhibited the growth of *Staph. aureus* at the MIC of 0.19 µg/ml and the MBC of 0.375 µg/ml (Table 13). Only samples 2-SNPs inhibited the growth of *Pseudomonas aeruginosa* at the MIC of 0.094 µg/ml and the MBC of 0.375 µg/ml. Both, samples 1-SNPs and 3-SNPs inhibited the growth of *Pseudomonas aeruginosa* at the MIC of 0.19 µg/ml and the MBC of 0.375 µg/ml (Table 14). So, the *Klebsiella pneumoniae* found to be more susceptible isolate to Ag NPs samples.

Statistical analysis performed to the absorption by taking the mean and standard deviation of MIC absorption for all four bacteria for each Ag NPs samples, described at (table 16&17) and histogram (figure 9).

Table 11: Minimum inhibitory concentration (MIC) of Ag NPs against *E. coli* by serial dilution plate count assay at wavelength = 590nm.

Concentration µg/ml / Sample	12	6	3	1.5	0.75	0.375	0.188	0.094	0.047	0.023	-ve control (media only)	+ve control (bacteria+ media)
1-Ag NPs	0.274	0.353	0.368	0.535	0.660	0.680	0.712	0.723	1.253	1.503	0.050	1.053
2-Ag NPs	0.260	0.267	0.314	0.399	0.489	0.691	0.718	0.728	1.337	1.533	0.050	1.042
3-Ag NPs	0.271	0.284	0.329	0.398	0.685	0.721	0.738	0.742	1.190	1.468	0.050	1.100

Table 12: Minimum inhibitory concentration (MIC) of Ag NPs against *Staph. aureus* MRSA by serial dilution plate count assay at wavelength = 590nm.

Concentration µg/ml / Sample	12	6	3	1.5	0.75	0.375	0.188	0.094	0.047	0.023	-ve control (media only)	+ve control (bacteria+ media)
1-Ag NPs	0.002	0.012	0.015	0.034	0.130	0.146	0.331	0.447	0.543	0.748	0.040	0.380
2-Ag NPs	0.013	0.043	0.051	0.064	0.087	0.170	0.254	0.302	0.634	0.675	0.040	0.558
3-Ag NPs	0.005	0.013	0.020	0.028	0.043	0.142	0.316	0.535	0.580	0.898	0.040	0.561

Table 13: Minimum inhibitory concentration (MIC) of Ag NPs against *Pseudomonas aeruginosa* by serial dilution plate count assay at wavelength = 590nm.

Concentration µg/ml / Sample	12	6	3	1.5	0.75	0.375	0.188	0.094	0.047	0.023	-ve control (media only)	+ve control (bacteria+ media)
1-Ag NPs	0.103	0.132	0.139	0.165	0.189	0.201	0.213	0.381	0.709	1.755	0.051	0.341
2-Ag NPs	0.014	0.025	0.029	0.037	0.051	0.060	0.069	0.185	0.443	0.941	0.051	0.297
3-Ag NPs	0.014	0.044	0.102	0.104	0.111	0.116	0.124	0.303	0.691	1.256	0.051	0.260

Table 14: Minimum inhibitory concentration (MIC) of Ag NPs against *Klebsiella pneumoniae* by serial dilution plate count assay at wavelength = 590nm.

Concentration µg/ml / Sample	12	6	3	1.5	0.75	0.375	0.188	0.094	0.047	0.023	-ve control (media only)	+ve control (bacteria+ media)
1-Ag NPs	0.004	0.013	0.017	0.020	0.044	0.045	0.053	0.075	0.229	0.577	0.035	0.535
2-Ag NPs	0.073	0.084	0.103	0.108	0.110	0.139	0.192	0.220	0.321	0.952	0.035	0.523
3-Ag NPs	0.002	0.006	0.011	0.012	0.022	0.024	0.075	0.122	0.286	0.858	0.035	0.533

Table 15: MIC detected by serial dilution plate count assay at wavelength=590nm.

Sample Tested bacteria	1-AgNPs	2-AgNPs	3-AgNPs
E. coli	0.723	0.728	0.742
S. aureus	0.331	0.302	0.535
P. aeruginosa	0.213	0.185	0.124
Klebsiella pneumoniae	0.229	0.321	0.286

Table 16: Descriptive Statistics for MIC experiment.

Sample	N	Mean	St Dev	SE Mean	95% CI for μ
1-Ag NPs	4	0.374	0.238	0.119	(-0.005, 0.753)
2-Ag NPs	4	0.384	0.237	0.119	(0.007, 0.761)
3-Ag NPs	4	0.422	0.272	0.136	(-0.012, 0.855)

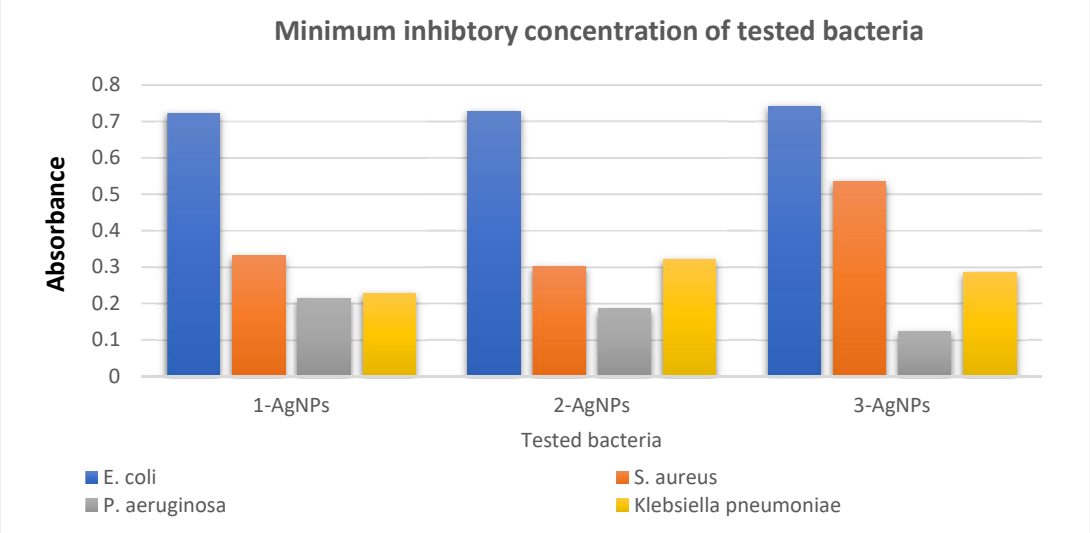

Fig. 9: Minimum inhibition concentrations of Ag NPs samples tested against gram-negative and gram-positive bacteria.

3.3.4. Antibiotic susceptibility testing

The data table (18) have shown that *Pseudomonas aeruginosa* was the most sensitive to antibiotic (Amikacin, Levofloxacin, ofloxacin, Gentamycin, Polymyxin B, Ciprofloxacin, Cefepime, Aztreonam, Piperacillin, Imipenem, Meropenem), while *Klebsiella pneumoniae* was the least sensitive only for Polymyxin B antibiotic with inhibition zone diameter 19mm. On the other hand, while *E. coli* was moderately sensitive to antibiotics (Amikacin, Gentamycin, Polymyxin B, Amoxicillin, Piperacillin, Imipenem, Meropenem, Tigecycline), and *Staphylococcus aureus* was moderately sensitive to antibiotics (Amikacin, Vancomycin, Linezolid, Teicoplanin, Doxycycline). It was found that all bacterial isolates were resistant to Ampicillin AMP, Co-Trimoxazole (Sulpha/Trimethoprim) COT, and cefoxitin CX antibiotics (table 19).

Table 17: Antibiotic susceptibility test for gram negative bacteria *E. coli, K. pneumonia,* and *P. aeruginosa.* R: resistant, S: sensitive, I: intermediate.

Antibiotic	1	2	3	4	5	6	7	8	9	10	11	12	13	14	15	16	17	18
Test bacteria	AK 30 (MMIZD)	EV 5 (MMIZD)	COT 25 (MMIZD)	OF 5 (MMIZD)	AMP 10 (MMIZD)	GEN 10 (MMIZD)	PB 300 (MMIZD)	CIP 5 (MMIZD)	FEP 30 (MMIZD)	AT 30 (MMIZD)	CX 30 (MMIZD)	CTR 30 (MMIZD)	AMC 30 (MMIZD)	CAZ 30 (MMIZD)	PIT 100/10 (MMIZD)	IPM 10 (MMIZD)	MRP 10 (MMIZD)	TGC 15 (MMIZD)
E. coli	20	13	-	-	-	19	12	16	-	11	-	11	18	-	30	30	30	20

	(S)	(R)	(R)	(R)	(R)	(S)	(S)	(R)	(R)	(R)	(R)	(R)	(S)	(R)	(S)	(S)	(S)	(S)
K. pneumonia	7 (R)	13 (R)	- (R)	- (R)	- (R)	10 (R)	19 (S)	- (R)	- (R)	- (R)	- (R)	- (R)	- (R)	- (R)	- (R)	16 (R)	16 (R)	17 (I)
P. aeruginosa	25 (S)	43 (S)	- (R)	30 (S)	- (R)	25 (S)	15 (S)	30 (S)	30 (S)	30 (S)	- (R)	- (R)	- (R)	- (R)	27 (S)	30 (S)	30 (S)	- (R)

Table 18: Antibiotic susceptibility test for gram positive bacteria *Staph. aureus MRSA*. R: resistant, S: sensitive, I: intermediate.

Antibiotic	**1**	**2**	**3**	**4**	**5**	**6**	**7**	**8**	**9**	**10**	**11**	**12**	**13**	**14**	**15**	**16**	**17**
Test bacteria	**AK 30 (MMIZD)**	**AMP 10 (MMIZD)**	**COT 25 (MMIZD)**	**LEV 5 (MMIZD)**	**OF 5 (MMIZD)**	**GEN 10 (MMIZD)**	**VA 30 (MMIZD)**	**A/S 10/10 (MMIZD)**	**AZM 15 (MMIZD)**	**LZ 30 (MMIZD)**	**CF 30 (MMIZD)**	**TEC 30 (MMIZD)**	**DO 30 (MMIZD)**	**E 15 (MMIZD)**	**CD 2 (MMIZD)**	**CX 30 (MMIZD)**	**CXM 30 (MMIZD)**
Staph. aureus MRSA	19 (S)	- (R)	12 (R)	19 (I)	13 (R)	12 (R)	16 (S)	- (R)	- (R)	25 (S)	- (R)	14 (S)	24 (S)	- (R)	19 (R)	- (R)	20 (R)

3.3.5. Microscopic analysis of antibacterial activity

The effects exerted by the Ag NPs *on* the cell shape and surface, the cell wall, the cytoplasmic membrane as well as on cell division and cell viability of *Pseudomonas aeruginosa* and *Staphylococcus aureus* are presented in Tables 19 &20.

Table 19: morphological effect of Ag NPs on *Pseudomonas aeruginosa* bacteria.

Morphological changes	**TEM**	
	Control	**Treated with Ag NPs**
Cell shape	Uniformly rod-shape	Cells are swollen and shrinked
Cell surface	Smooth cell surface	Rough cell surface
Cytoplasmic membrane	Cytoplasm was homogenously electron dense	Partial loss of cytoplasmic electron density
Cell wall	Intact	Cell wall distortion
Cell viability	Viable	Cell death

Table 20: Morphological effect of Ag NPs on *Staphylococcus aureus* bacteria.

Morphological changes	**TEM**	
	Control	**Treated with Ag NPs**
Cell shape	Uniformly grape shape (round)	Cells are swollen and shrinked
Cell surface	Smooth cell surface	Rough cell surface
Cytoplasmic membrane	Cytoplasm was homogenously electron dense	Partial loss of cytoplasmic electron density
Cell wall	Intact	Cell wall distortion
Cell viability	Viable	Cell death

Pseudomonas aeruginosa and *Staphylococcus aureus* treated with 2-Ag NPs and 3-Ag NPs samples showed size-dependent morphological changes that increased in severity as the size of the decreased (Fig. 10 &11). Under normal conditions the cells of *Pseudomonas aeruginosa* under the transmission Electron Microscopy (TEM) were uniformly rod-shaped and had smooth cell surfaces

(Table 19 and Fig. 10 A, B). Interaction with sample 2-AgNPs (Fig. 10 D) Ag NPs inter the cell and condensed inside the cell resulted in shrinkage of the cell completely worn-out cell walls and cytoplasmic membrane caused morphological changes in the cell wall visualized as membrane corrugations, swelling and increase the membrane permeability in comparison with the control (Fig. 10 A, B and C). Interaction with sample 3-Ag NPs (Fig. 10 E); showed major structural changes on the cell wall, cell swelling and rupture then loss of intracellular material, cell organelles damage that led to cell death, and (Fig. 10 F); cell loss the original shape causing roughness of the cell and loss of cytoplasmic density. While the cells of *Staphylococcus aureus* Under normal conditions under the Transmission Electron Microscopy (TEM) were Uniformly grape shape (round) and had Smooth cell surface (Table 20 and Fig. 11 A, B, C). (Fig. 11 E-K) showed major structural changes on the cell wall (irregular and roughness of cell) cause loss of cytoplasmic density, not complete budding process due to the effect of Ag NPs, also noticeable damage in cell wall, cell membrane and cytoplasmic component. the Grape-like of *Staphylococcus aureus* seen surrounded with Ag NPs and Ag NPs inter inside the cell lead to damage plasma membrane and the intracellular component get out the cell.

The effects of Ag NPs on the morphology of the bacterial cells examined using TEM also confirmed the damaging effects of the plant extract on the bacterial cell structure (Table 19 and 20). Figures 10 and 11 show how nanoparticles remain attached in spherical form after cells were lysed completely.

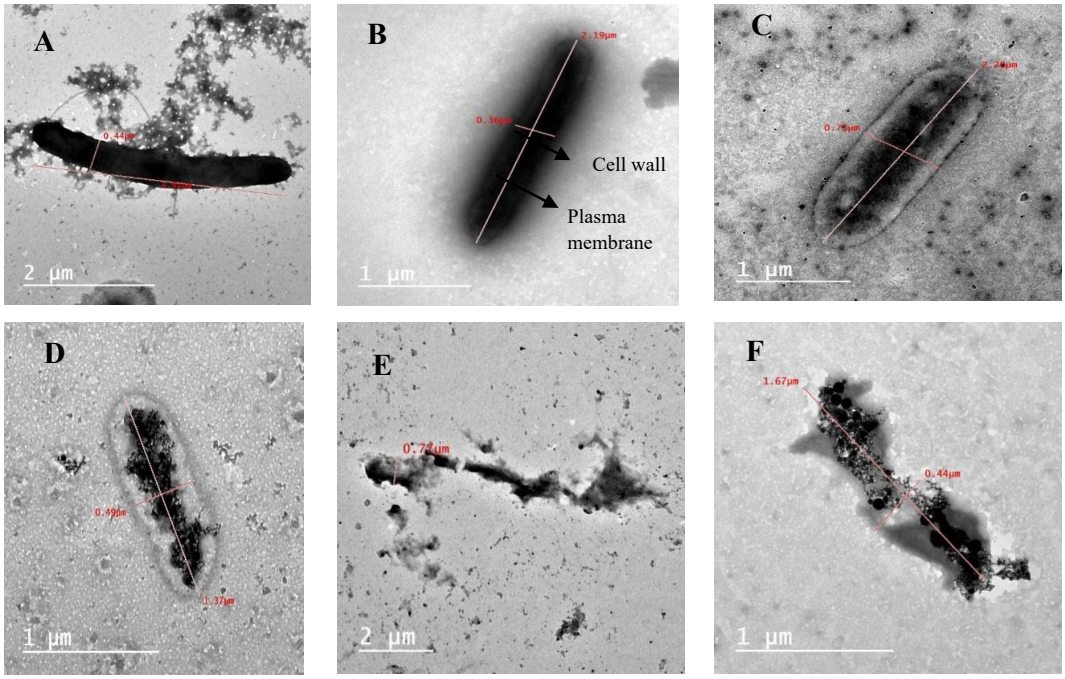

Fig. 10: TEM images of a *Pseudomonas aeruginosa* sample at different magnifications are shown. (A) and (B) Control sample, i.e. no silver nanoparticles were used; (C) Control sample, i.e. no silver nanoparticles were used but the plasma membrane shrinkage because fixation with glutaraldehyde; (D) samples that were previously treated with sample 2-Ag NPs. Silver nanoparticles can be inter inside the bacteria and noticeable damage in the cell membrane and cell wall can be seen when compared with the control sample; (E) and (F) samples that were previously treated with sample 3-Ag NPs; Fig (E) cell swelling and rupture then loss of intracellular material; (F) cell loss the original shape causing roughness of the cell and loss of cytoplasmic density.

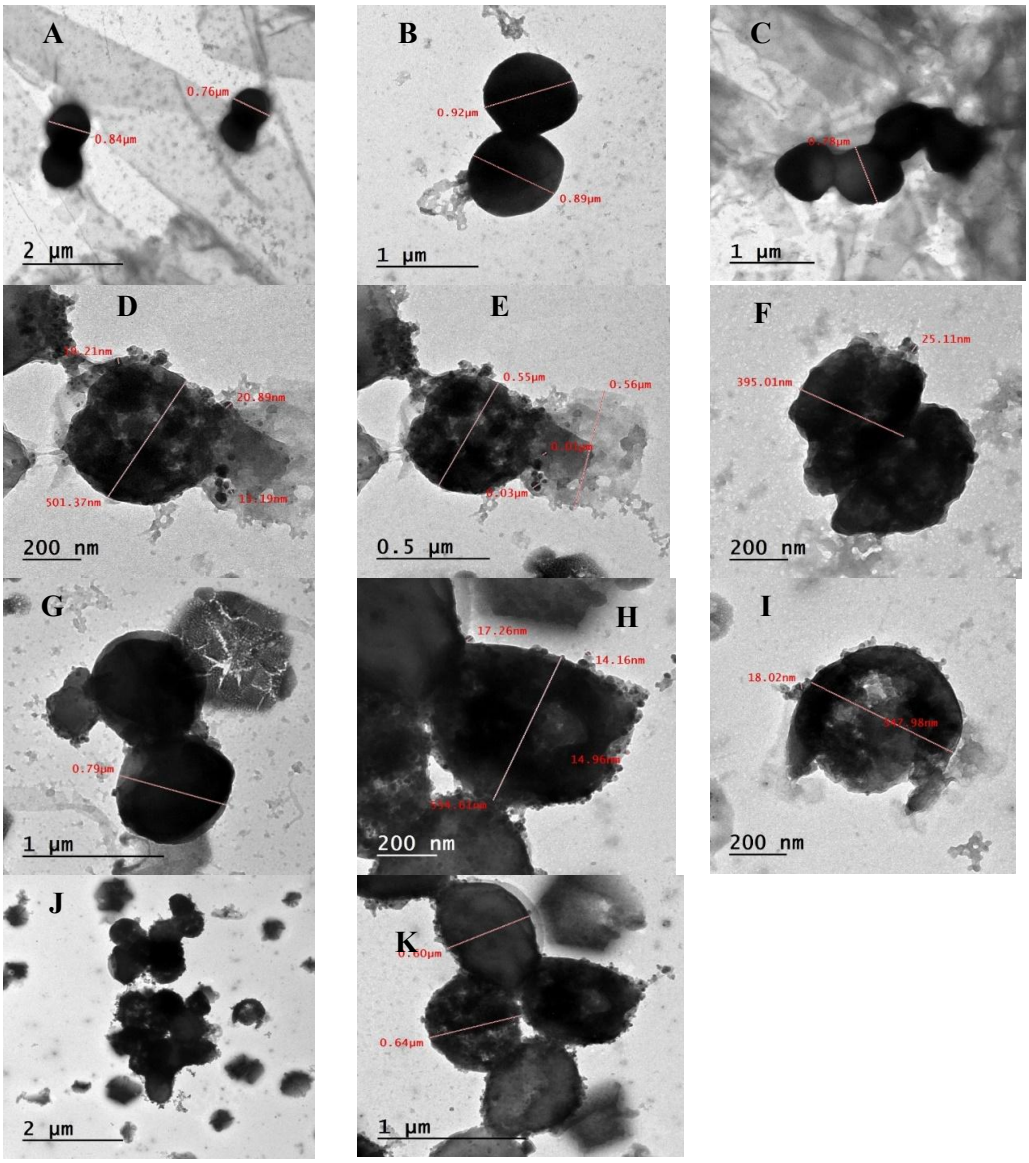

Fig 11: TEM images of a *Staphylococcus aureus* sample at different magnifications are shown. (A), (B) and (C) Control sample, i.e. no silver nanoparticles were used; (D)- (G) samples that were previously treated with sample 2-Ag NPs; (D) and (E) Silver nanoparticles inter inside the bacterial cell and noticeable damage in cell membrane, cytoplasmic component, and the cell wall can be seen when compared to the control sample; (F) Irregular cell wall, not complete budding process and noticeable damage in cell wall, cell membrane and cytoplasmic component; (G) noticeable damage in cell wall, cytoplasmic component and shrinkage in cell membrane; (H)- (K) samples that were previously treated with sample 3-Ag NPs; (H) Ag NPs surround and attach to the cell wall and also inter inside the cell and damage the cytoplasmic component; (I) Ag NPs inter the cell causing cell swelling rupture and loss of intracellular material; (J) and (K) Grape-like of *Staphylococcus aureus* seen surrounded with Ag NPs and Ag NPs inter inside the cell lead to damage plasma membrane and the intracellular component get out the cell.

4. Discussion

Ag NPs synthesized greenly by *citrus paradisi* extract, the appearance of yellowish-brown color indicating Presence of Ag NPs due to excitation of surface plasmon vibrations (Rai *et al.,* 2006). It is known that the extracts of plants, fruits, and vegetables contain secondary metabolites such as flavonoids, phenolic acids, terpenoids, and alkaloids. These molecules contain hydroxyl groups which

are used to carry out the redox reactions that are responsible for the synthesis of Ag NPs since they are involved in the reduction of silver ions into metallic silver atoms which then agglomerate and grow to form nanostructures (Manosalva *et al., 2019).* Much of the flavonoids in citrus are flavanones bound together as glycosides. In the orange and tangerine peel, hesperidin predominates; in grapefruit, naringin and narirutin stand out; finally, eriocitrin and hesperidin stand out in lemon and lime (Rafique *et al., 2017;* Montanari *et al.,* 1998). The Ag-NPs were characterized by UV-vis spectroscopy, is the most important technique to assess the surface Plasmon resonance of the formed nanoparticles as the presences of sharp absorption band indicates that the formation of silver nanoparticles (Gurunathan *et al.,* 2014). UV-vis spectra show an optical absorption narrow band peak at 205 nm, 205, and 205 nm. Interestingly, 1-Ag NPs display broad band at 260nm that may be due to non-homogenous size distribution of the prepared colloid. These maxima absorption bands around 200nm for the prepared nano-formulations agreed with Paramelle *et al.,* (2014). The variations in the values of absorbance between the prepared formulations may attributed to the particle size, shape variations or number of nanoparticles formed (Banerjee *et al.,* 2014). As a result, (Fig. 3) The size distribution of the prepared silver nano-formulation and their average particles hydrodynamic size were determined via DLS. Also, DLS results displayed the polydispersity index (PDI) of nano-formulations, which correlates with their size homogeneity distribution. The higher the PDI value indicates less size homogeneity of the colloidal nanoparticles (Singh, 2022). The negative zeta potential value (Fig. 4) further confirms the stability of nanoparticles in aqueous solutions (Parveen *et al.,* 2021). The negative zeta potential value depicted by the silver nanoparticles may be due to the potential capping of the bioorganic components present in the plant's extracts (Edison and Sethuraman, 2012). The high negative values reveal the electrostatic repulsion between the particles and facilitate the achievement of stable silver nanoparticles without any agglomeration (Sivaraman *et al.,* 2013).

The TEM images of the silver nanoparticles are shown in Fig. 5. The surface morphology of silver nanoparticles showed even shape and spherical nature. In the present study, the histogram of the particle the mean size ranges from 5.89 to 19.76nm. Similar results were also consistent for Ag NPs synthesized by Grapefruit's peel through a simple green and eco-friendly route. Aqueous extract of Grapefruit's peel was used synthesize nano silver. The size of nanoparticle was determined at 5-65 nm (Faghihi *et al.,* 2020). Electron diffraction EDX (Fig. 5) confirmed the spherical crystalline nature of the prepared nano-formulations Kurian *et al.,* 2016. This result strongly confirms that *Citrus paradisi* peel extract might act as a reducing and capping agent in the production of silver nanoparticles.

Esposito *et al.,* (2016) reported that the most common organisms that are involved in community acquired Skin and soft tissue infections include gram-positive cocci-like *Staphylococcus aureus*, and Buhl *et al.,* (2015) reported that recently Gram-negative bacteria, such as *Escherichia coli* and *pseudomonas aeruginosa* started to be an emerging pathogen that affect morbidity and mortality in skin and soft tissues. Ahmed *et al.,* (2020) isolate *Klebsiella* species from Skin and soft tissue infections patients. In the present study the *Klebsiella pneumoniae* the least sensitive to antibiotics (table 19), these results consistent with Ahmed *et al.,* (2020) Klebsiella spp. was the most resistant isolated Gram-negative bacteria to antibiotics.

Bactericidal activities of biosynthesized Ag NPs revealed that the inhibition was comparatively higher than plant extract. It inhibited Gram-positive and Gram-negative bacteria very efficiently (Table 7 and 9; Fig. 7 and 8). The inhibition zone of Ag NPs synthesized using citrus sinensis observed in case of *E. coli*, *Staphylococcus aureus*, and *Pseudomonas aeruginosa* was lower than the present study (Kaviya *et al.,* 2011). The results obtained by well diffusion tests were in good agreement with the microdilution tests, show that the *Pseudomonas aeruginosa* found to be less susceptible to Ag NPs (Fig. 9; Table 7 &13) with MIC 0.19 µg/mL higher than the other bacteria, while in decreasing concentration to 0.094 µg/mL inhibit the growth of *E. coli* and *Staphylococcus aureus*, *Klebsiella pneumoniae* the most effective bacteria at MIC 0.047 µg/mL (Table 14) and highest inhibition zone (Table 7) it is consistent with Chandrasekharan *et al.* (2022) demonstrated the *Gmelina arborea* mediated Ag NPs (GA-Ag NPs) against *P. aeruginosa* and *E. coli*. The authors showed that the GA-Ag NPs exert MIC and MBC value 90 µg/mL against *P. aeruginosa*, and 20 µg/mL of MIC and 40 µg/mL of MBC value against *E. coli* which is higher than the present study. According to Masri *et al.,* (2018) using antibacterial assays, the effects of drugs alone and drugs-conjugated with silver nanoparticles were tested against a variety of Gram-negative and Gram-positive bacteria including neuropathogenic

Escherichia coli, *Pseudomonas aeruginosa*, *Klebsiella pneumoniae*, *Staphylococcus aureus* and show inhibitory effect the same as the present study.

The growth of all bacteria decreased and inhibited after24h of incubation even in the presence of Ag NPs at concentration of 24 µg/mL at well and disc diffusion methods. Similar results were observed by Shivaji *et al.* (2011), when higher concentrations (10 and 20µg/mL) of Ag NPs completely inhibited Gram positive and negative bacteria within 20h.

Both *Staphylococcus aureus* and *Pseudomonas aeruginosa* treated with samples 2-Ag NPs and 3-Ag NPs, at Fig. 10 &11 show changes in outer cell wall of the cell at sample 2-Ag NPs and show intracellular changes at sample 3-Ag NPs, this is consistent with Inphonlek *et al.,* 2010 &Xiu *et al.,* 2012 studies revealed that the NPs greater than 10nm accumulate on the cellular surface and compromise cellular permeability; however, NPs smaller than 10nm penetrate into the bacteria, affecting DNA and the enzymes leading to cellular death. Silver is positively charged and thus tends to react with negatively charged biomolecules such as phosphorous and sulfur, which are the main components of the cell membrane, proteins, and DNA bases. Silver nanoparticles damage the cell wall and membrane of bacterial cells, causing various morphological changes (Hamouda *et al.,* 2019). Several studies have shown the effective use of silver nanoparticles against Gram-positive and Gram-negative pathogens (Mukundan *et al., 2017)*. The critical characteristics of nanoparticles are a size that must be in the field of 1–100 nm, and they also possess an excellent surface volume ratio and shape of the nanoparticles. All of these factors play a vital role (Huh & Kwon,2011). The size of the nanoparticles plays an important role in antibacterial activity. The various studies demonstrates that the smaller the dimension of the nanoparticle, the greater is the ability to penetrate the bacteria (Loo *et al.,* 2018; Bruna *et al., 2021;* Yin *et al.,* 2020; Kalwar & Shan, 2018).

Silver ions are continuously released from silver nanoparticles, which may consider a mechanism for killing microbes. Silver ions can easily adhere to the cell wall and cytoplasmic membrane as they are more closely related to sulfur proteins and also due to electrostatic attraction (Liu *et al., 2021;* Shaikh *et al., 2019;* Wahab *et al., 2021;* Mendes *et al., 2022;* Ahmad *et al., 2020;* Xu *et al., 2020;* Jin *et al., 2023)*. At the same time, the bacterial envelope is disrupted because when silver ions attach to the cell wall or cytoplasmic membrane, it enhances the permeability of the cell and ultimately leads to cell disruption. When free silver ions are uptake by cells, they deactivate respiratory enzymes, generating reactive oxygen species interrupting adenosine triphosphate production. ROS is the principal species that provokes the activity of DNA modification and cell membrane disruption. In DNA, sulfur and phosphate are essential components. Still, the interaction of Ag NPs with sulfur and phosphorus in DNA can cause difficulties in DNA replication and cell reproduction or even result in the termination of bacteria. Sometimes, the ribosome's denaturation in the cytoplasm occurs as the silver ions can inhibit protein synthesis (Dakal *et al., 2016;* Arif & Uddin, 2021). Ag NPs garner in the pit once they are attached to the cell surface (Liao *et al., 2019)* and a cell membrane's denaturation occurs due to the accumulation of Ag NPs. They also can enter the cell wall and alter the structure of the cell membrane due to their nanoscale size (Liao *et al., 2019)*. Denaturation of the cytoplasmic membrane also causes cell rupture leading to cell lysis. Ag NPs are also involved in bacterial signal transduction. Phosphorylation of protein substrate and nanoparticles can dephosphorylate tyrosine residues on peptide substrates, ultimately affecting the signal transduction in bacteria. Disruption in signal transduction can escort cell apoptosis and termination of cell multiplication (Liu *et al., 2021*; Qing *et al., 2018)*.

The antimicrobial efficiency of Ag NPs is more against Gram-negative than Gram-positive bacteria (Meikle *et al., 2020)*. Gram-negative bacteria have a thick Lipopolysaccharide LPS layer in their cell wall with a thin peptidoglycan layer. In contrast, Gram-positive bacterial cell walls contain thin LPS and thick peptidoglycan layers. The cellular wall made of a thick peptidoglycan layer reduces the chances of Ag NP penetration into cells (Meikle *et al., 2020)*. The uptake of Ag NPs is significant for the antibacterial effect, as it has been demonstrated on various Gram-positive and Gram-negative bacteria (Noronha *et al., 2017)*. According to different reports, it is suggested that the relatively small NPs smaller than 10 nm can penetrate easily inside the bacterial cell and ultimately cause cell lysis (Saravanan *et al., 2018)*. The interaction of Ag+ ions with biological macromolecules such as enzymes and DNA based on electron discharge or free radical generation are some other mechanisms of action of Ag+ ions or Ag NPs for the deactivated (Sharma *et al., 2009)*.Alternation in protein synthesis and cell wall synthesis, evidenced by amassing of enveloped protein precursor or disruption of the outer

cellular membrane, leading to ATP leakage, are also demonstrated to pave a significant role in the antimicrobial activity of Ag NPs (Park *et al., 2011)*. In addition, the role of nanoparticle shape concerning their antimicrobial potential has also been demonstrated. Ali Bakhtiari-standard et al. synthesized Ag NPs in spherical shape shows excellent antimicrobial activity. They tested NPs against *E. coli* and *S. aureus*. *E. coli,* and they observed that *E. coli* is more susceptible than *S. aureus*. (Burda *et al., 2005).* From the various studies on MDR bacteria, Ag NPs are effective against those pathogenic bacteria such as *E. coli*, *S. Typhi*, *S. epidermidis* and, *S. aureus*, *P. aeruginosa* (Seppälä *et al., 1997).* The adhesion and accumulation of Ag NPs on the cell surface were especially observed for Gram-negative bacteria. Ag NPs can penetrate bacterial cells through a water-filled channel called porins in the outer membrane of Gram-negative bacteria. Porins are primarily involved in passively transporting hydrophilic molecules of various sizes and charges across the membrane. It is likely that that the thicker cell wall of Gram-positive bacteria produces the penetration of silver ions into the cytoplasm, therefore the effect of Ag NPs is more pronounced in Gram-negative bacteria than in Gram-positive bacteria (Chauhan *et al., 2016)*. It is also possible that the presence of lipopolysaccharides contributes to the structural integrity of the Gram-negative bacteria cell wall, making such bacteria more sensitive to silver nanoparticles because the negative charge of the lipopolysaccharides promotes Ag NP adhesion (Pal *et al., 2007)*. Some researchers have assumed that the ability of silver nanoparticles to attach to the bacterial cell wall due to the electrostatic interaction between positively charged silver ions and the negatively charged surface of the cell membrane because of the carboxyl, phosphate, and amino groups, give an opportunity to subsequently penetrate it, thereby causing structural changes in the cell membrane and, as a result, its permeability. Then, dissipation of proton motive force (PMF) and thus membrane destruction occurs (Netala *et al., 2015;* Rashid *et al., 2017*). Ag NPs may also act as a carrier to transport Ag^+ more efficiently to bacteria cells whose proton motive force would consequently reduce the local pH and increase Ag^+ release (Ovais *et al., 2016*). In addition, it is believed that silver nanoparticles form free radicals upon contact with bacteria that damage the cell membrane, making it porous (Singh *et al., 2016)*.

However, other researchers are of the opinion that Ag NPs adhere to the surface of bacteria and change the membrane properties, while inside the bacterial cell, they can lead to DNA damage (Reidy *et al., 2013;* Durán *et al., 2016).* For example, the review of MaQuillan et al. suggests that the primary mechanism of action of silver nanoparticles is cell membrane dissolution (McQuillan *et al., 2012)*. In addition, the dissolution of silver nanoparticles releases antimicrobial silver ions, which can interact with thiol-containing proteins in the cell wall and influence their functions. When interacting with the outer membrane, silver nanoparticles can bind to proteins, forming complexes with electronic donors containing oxygen, phosphorus, nitrogen, or sulfur atoms. It is the interaction with thiol groups that is best described in the literature. Thus, silver nanoparticles lead to the inactivation of membrane-bound enzymes and proteins by interaction with disulfide-bonds and active site blocking (Holt *et al., 2005)*. Reportedly, Ag NPs have the possibility of increasing the trans/cis ratio of unsaturated membrane fatty acids, which leads to changes in membrane fluidity and the composition of the lipid bilayer. It can lead to changes in the membrane structure that can prevent the membrane functioning, causing an increase in permeability and loss of membrane integrity (Mikhailova,2020).

5. Conclusion

The antibacterial properties of Ag NPs and the effect of *Citrus paradisi* peel extract on the structure and the antibacterial effectiveness were investigated against bacteria isolate from soft tissue infecting-patients. Antibacterial effect of silver nanoparticles samples increased with the decreasing of size of silver nanoparticles. The results of this study also suggested that the smaller nanoparticles enhance the inhibition of bacteria than the larger one. These results suggest that Ag NPs greenly synthesized via *Citrus paradisi* peel extract (Grapefruit) could be used as an adjuvant for the treatment of soft tissue infection caused by Gram-negative and Gram-positive bacteria. Thus, our findings support the claim that Ag NPs have considerable effective antibacterial activity, which can be used to enhance the action of existing anti biotics against Gram-negative and Gram-positive bacteria.

References

Abbaszadegan, A., Y. Ghahramani, A. Gholami, B. Hemmateenejad, S. Dorostkar, M. Nabavizadeh, and H. Sharghi, 2015. The effect of charge at the surface of silver nanoparticles on antimicrobial activity against gram-positive and gram-negative bacteria: a preliminary study. Journal of Nanomaterials, 2015.

Adamis, G., M.G. Papaioannou, E.J. Giamarellos-Bourboulis, P. Gargalianos, J. Kosmidis, and H. Giamarellou, 2004. Pharmacokinetic interactions of ceftazidime, imipenem and aztreonam with amikacin in healthy volunteers. International journal of antimicrobial agents, 23(2): 144-149.

Ahmad, S.A., S.S. Das, A. Khatoon, M.T. Ansari, M. Afzal, M.S. Hasnain, and A.K. Nayak, 2020. Bactericidal activity of silver nanoparticles: A mechanistic review. Materials Science for Energy Technologies, 3: 756-769.

Ahmed, F., R. Bassyouni, and Y. Zedan, 2020. Bacteriological Profile of Bacteria isolated from Skin and Soft Tissue Infections. Fayoum University Medical Journal, 7(1): 41-51.

Ahsman, M.J., E.D. Wildschut, Tibboel, D., and R.A. Mathot, 2010. Pharmacokinetics of cefotaxime and desacetyl cefotaxime in infants during extracorporeal membrane oxygenation. Antimicrobial Agents and Chemotherapy, 54(5): 1734-1741.

Aljuffali, I., Huang, C.H., and J.Y. Fang, 2015. Nanomedical strategies for targeting skin microbiomes. Current drug metabolism, 16(4): 255-271.

Amparo, T.R., J.B. Seibert, P.M.D.A. Vieira, L.F.M. Teixeira, O.D.H.D. Santos, and G.H.B. de Souza, 2020. Herbal medicines to the treatment of skin and soft tissue infections: advantages of the multi-targets action. Phytotherapy Research, 34(1): 94-103.

Arif, R., and R. Uddin, 2021. A review on recent developments in the biosynthesis of silver nanoparticles and its biomedical applications. Medical Devices & Sensors, 4(1): e10158.

Atlas, R., 2010. Handbook of microbiological media. 4th Education. In Library of Congress Cataloging-in-Publication Data. New York. USA.

Banerjee, P., M. Satapathy, A. Mukhopahayay, and P. Das, 2014. Leaf extract mediated green synthesis of silver nanoparticles from widely available Indian plants: synthesis, characterization, antimicrobial property and toxicity analysis. Bioresources and Bioprocessing, 1: 1-10.

Baron S., 1996. Medical microbiology (4th ed.). University of Texas Medical Branch at Galveston.

Bergey, D.H., 1994. Bergey's manual of determinative bacteriology. Lippincott Williams & Wilkins.

Betts, J.W., M. Hornsey, and R.M. La Ragione, 2018. Novel antibacterials: alternatives to traditional antibiotics. In Advances in microbial physiology (73:123-169). Academic Press.

Breakwell, D., B. MacDonald, C. Woolverton, K. Smith, and R. Robison, 2007. Colony morphology protocol. American Society for Microbiology, 1-7.

Bruna, T., F. Maldonado-Bravo, P. Jara, and N. Caro, 2021. Silver nanoparticles and their antibacterial applications. International Journal of Molecular Sciences, 22(13): 7202.

Buhl, M., S. Peter, and M. Willmann, 2015. Prevalence and risk factors associated with colonization and infection of extensively drug-resistant Pseudomonas aeruginosa: a systematic review. Expert review of anti-infective therapy, 13(9): 1159-1170.

Burda, C., X. Chen, R. Narayanan, and M.A. El-Sayed, 2005. Chemistry and properties of nanocrystals of different shapes. Chemical reviews, 105(4): 1025-1102.

Chandrasekharan, S., G. Chinnasamy, and S. Bhatnagar, 2022. Sustainable phyto-fabrication of silver nanoparticles using Gmelina arborea exhibit antimicrobial and biofilm inhibition activity. Scientific Reports, 12(1): 156.

Chauhan, N., A.K. Tyagi, P. Kumar, and A. Malik, 2016. Antibacterial potential of Jatropha curcas synthesized silver nanoparticles against food borne pathogens. Frontiers in microbiology, 7:1748.

Clebak, K.T., and M.A. Malone, 2018. Skin infections. Primary Care: Clinics in Office Practice, 45(3): 433-454.

CLSI, Performance Standards for Antimicrobial Disk Susceptibility Tests; Approved Standard—Eleventh Edition. CLSI document M02-A11. Clinical and Laboratory Standards Institute, 950 West Valley Road, Suite 2500, Wayne, Pennsylvania 19087 USA, 2012.

Cockerill, F.R., M.A. Wikler, K. Bush, M. Dudley, G. Eliopoulos, and D. Hardy, 2010. Performance standards for antimicrobial susceptibility testing; twentieth informational supplement M100-S20. Clinical and Laboratory Standards Institute: Wayne, PA, USA.

Collee, J.G., W. Marr, Specimen collection, J.G. Collee, A.G. Fraser, B.P. Marmion, A. Simmons, editors. Mackie and McCartney's, 2012. culture containers & media. In Practical Medical Microbiology, 95-111.

Dakal, T.C., A. Kumar, R.S. Majumdar, and V. Yadav, 2016. Mechanistic basis of antimicrobial actions of silver nanoparticles. Frontiers in microbiology, 7: 1831.

Durán, N., M. Durán, M.B. De Jesus, A.B. Seabra, W. J. Fávaro, and G. Nakazato, 2016. Silver nanoparticles: A new view on mechanistic aspects on antimicrobial activity. Nanomedicine: nanotechnology, biology and medicine, 12(3): 789-799.

Edison, T.J.I., and M.G. Sethuraman, 2012. Instant green synthesis of silver nanoparticles using Terminalia chebula fruit extract and evaluation of their catalytic activity on reduction of methylene blue. Process Biochemistry, 47(9): 1351-1357.

Elamawi, R.M., R.E. Al-Harbi, and A.A. Hendi, 2018. Biosynthesis and characterization of silver nanoparticles using Trichoderma longibrachiatum and their effect on phytopathogenic fungi. Egyptian journal of biological pest control, 28(1): 1-11.

Esposito, S., S. Noviello, and S. Leone, 2016. Epidemiology and microbiology of skin and soft tissue infections. Current opinion in infectious diseases, 29(2): 109-115.

Faghihi, R., K. Larijani, V. Abdossi, and P. Moradi, 2020. Silver nanoparticles produced by green synthesis using Citrus paradise peel inhibits Botrytis cinerea in vitro. Journal of Horticulture and Postharvest Research, 3(2): 151-160.

Fathy, M.M., 2020. Biosynthesis of silver nanoparticles using thymoquinone and evaluation of their radio-sensitizing activity. BioNanoScience, 10(1): 260-266.

Fozouni, L., S. Javidmehr, H. Barghamadi, A. Mazandarani, and S. Rouhafza, 2019. Antibacterial Effect of Zinc Oxide Nanoparticles on Group A β-Hemolytic Streptococci with Macrolide Resistance Isolated from University Student Carriers in North of Iran. International Journal of Infection, 6(1).

Gopinath, V., D. MubarakAli, S. Priyadarshini, N.M. Priyadharsshini, N. Thajuddin, and P. Velusamy, 2012. Biosynthesis of silver nanoparticles from Tribulus terrestris and its antimicrobial activity: a novel biological approach. Colloids and surfaces B: Biointerfaces, 96: 69-74.

Gurunathan, S., J.W. Han, D.N. Kwon, and J.H. Kim, 2014. Enhanced antibacterial and anti-biofilm activities of silver nanoparticles against Gram-negative and Gram-positive bacteria. Nanoscale research letters, 9: 1-17.

Hamouda, R.A., M. Abd El-Mongy, and K.F. Eid, 2019. Comparative study between two red algae for biosynthesis silver nanoparticles capping by SDS: Insights of characterization and antibacterial activity. Microbial pathogenesis, 129: 224-232.

Harley. J.P., 2005. Laboratory exercises in microbiology, 6th Ed, New York: The McGraw− Hill.

Harrigan, W.F., and M.E. McCance, 1966. Laboratory methods in microbiology Academic Press. London and New york, 51.

Hemraj, V., Diksha, S., and Avneet, G. 2013. A review on commonly used biochemical test for bacteria. Innovare J. Life Sci., 1(1): 1-7.

Holt, K.B., and A.J. Bard, 2005. Interaction of silver (I) ions with the respiratory chain of Escherichia coli: an electrochemical and scanning electrochemical microscopy study of the antimicrobial mechanism of micromolar Ag+. Biochemistry, 44(39):13214-13223.

Huh, A.J., and Y.J. Kwon, 2011. "Nanoantibiotics": a new paradigm for treating infectious diseases using nanomaterials in the antibiotics resistant era. Journal of controlled release, 156(2): 128-145.

Inphonlek, S., N. Pimpha, and P. Sunintaboon, 2010. Synthesis of poly (methyl methacrylate) core/chitosan-mixed-polyethyleneimine shell nanoparticles and their antibacterial property. Colloids and Surfaces B: Biointerfaces, 77(2): 219-226.

Jackson, T.C., T.O. Uwah, N.L. Ifekpolugo, and N.A. Emmanuel, 2018. Comparison of antimicrobial activities of silver nanoparticles biosynthesized from some Citrus species. American Journal of Nano Research and Applications, 6(2): 54-59.

Jin, J., Y. Wu, L. Liang, Y. Wei, X. Zheng, and Y. Chen, 2023. Altering sliver nanoparticles-induced inhibition to bacterial denitrification via visible light by regulating silver transformation and adaptive mechanism under anaerobic conditions. Chemical Engineering Journal, 452: 139268.

Jonasson, E., E. Matuschek, and G. Kahlmeter, 2020. The EUCAST rapid disc diffusion method for antimicrobial susceptibility testing directly from positive blood culture bottles. Journal of Antimicrobial Chemotherapy, 75(4): 968-978.

Kalwar, K., and D. Shan, 2018. Antimicrobial effect of silver nanoparticles (AgNPs) and their mechanism–a mini review. Micro & Nano Letters, 13(3): 277-280.

Kaviya, S., J. Santhanalakshmi, B. Viswanathan, J. Muthumary, and K. Srinivasan, 2011. Biosynthesis of silver nanoparticles using Citrus sinensis peel extract and its antibacterial activity. Spectrochimica Acta Part A: Molecular and Biomolecular Spectroscopy, 79(3): 594-598.

Klamm, L.S., 2019. Klamm's Microbiology Laboratory Manual.

Kovács, N. 1956. Identification of Pseudomonas pyocyanea by the oxidase reaction. Nature (London) 178:703.

Lee, N.Y., W.C. Ko, and P.R. Hsueh, 2019. Nanoparticles in the treatment of infections caused by multidrug-resistant organisms. Frontiers in pharmacology, 10: 1153.

Liao, C., Y. Li, and S.C. Tjong, 2019. Bactericidal and cytotoxic properties of silver nanoparticles. International journal of molecular sciences, 20(2):449.

Liao, S., Y. Zhang, X. Pan, F. Zhu, C. Jiang, Q. Liu, ... and L. Chen, 2019. Antibacterial activity and mechanism of silver nanoparticles against multidrug-resistant Pseudomonas aeruginosa. International Journal of Nanomedicine, 14: 1469.

Liu, X., J.L. Chen, W.Y. Yang, Y.C. Qian, J.Y. Pan, C.N. Zhu, ... and D.P. Zhang, 2021. Biosynthesis of silver nanoparticles with antimicrobial and anticancer properties using two novel yeasts. Scientific Reports, 11(1): 15795.

Loo, Y.Y., Y. Rukayadi, M.A.R. Nor-Khaizura, C.H. Kuan, B.W. Chieng, M. Nishibuchi, and S. Radu, 2018. In vitro antimicrobial activity of green synthesized silver nanoparticles against selected gram-negative foodborne pathogens. Frontiers in Microbiology, 9:1555.

Manosalva, N., G. Tortella, M. Cristina Diez, H. Schalchli, A.B. Seabra, N. Durán, and O. Rubilar, 2019. Green synthesis of silver nanoparticles: effect of synthesis reaction parameters on antimicrobial activity. World Journal of Microbiology and Biotechnology, 35: 1-9.

Masri, A., A. Anwar, D. Ahmed, R.B. Siddiqui, M. Raza Shah, and N.A. Khan, 2018. Silver nanoparticle conjugation-enhanced antibacterial efficacy of clinically approved drugs cephradine and vildagliptin. Antibiotics, 7(4): 100.

McQuillan, J.S., H. Groenaga Infante, E. Stokes, and A.M. Shaw, 2012. Silver nanoparticle enhanced silver ion stress response in Escherichia coli K12. Nanotoxicology, 6(8): 857-866.

Meikle, T.G., B.P. Dyett, J.B. Strachan, J. White, C.J. Drummond, and C.E. Conn, 2020. Preparation, characterization, and antimicrobial activity of cubosome encapsulated metal nanocrystals. ACS Applied Materials & Interfaces, 12(6): 6944-6954.

Mendes, C.R., G. Dilarri, C.F. Forsan, V. D. M. R. Sapata, P.R.M. Lopes, P.B. de Moraes, ... and E.D. Bidoia, 2022. Antibacterial action and target mechanisms of zinc oxide nanoparticles against bacterial pathogens. Scientific Reports, 12(1): 2658.

Mikhailova, E.O., 2020. Silver nanoparticles: Mechanism of action and probable bio-application. Journal of functional biomaterials, 11(4): 84.

Moffarah, A.S., M.A. Mohajer, B.L. Hurwitz, and D.G. Armstrong, 2016. Skin and soft tissue infections. Diagnostic Microbiology of the Immunocompromised Host, 691-708.

Mohammed, A.E., 2015. Green synthesis, antimicrobial and cytotoxic effects of silver nanoparticles mediated by Eucalyptus camaldulensis leaf extract. Asian Pacific Journal of Tropical Biomedicine, 5(5): 382-386.

Montanari, A., J. Chen, and W. Widmer, 1998. Citrus flavonoids: a review of past biological activity against disease: discovery of new flavonoids from Dancy tangerine cold pressed peel oil solids and leaves. Flavonoids in the living system, 103-116.

Mukundan, D., R. Mohankumar, and R. Vasanthakumari, 2017. Comparative study of synthesized silver and gold nanoparticles using leaves extract of Bauhinia tomentosa Linn and their anticancer efficacy. Bulletin of Materials Science, 40: 335-344.

Mussin, J., V. Robles-Botero, R. Casañas-Pimentel, F. Rojas, L. Angiolella, E. San Martin-Martinez, and G. Giusiano, 2021. Antimicrobial and cytotoxic activity of green synthesis silver nanoparticles targeting skin and soft tissue infectious agents. Scientific reports, 11(1): 14566.

Netala, V.R., V.S. Kotakadi, V. Nagam, P. Bobbu, S.B. Ghosh, and V. Tartte, 2015. First report of biomimetic synthesis of silver nanoparticles using aqueous callus extract of Centella asiatica and their antimicrobial activity. Applied Nanoscience, 5: 801-807.

Noronha, V.T., A.J. Paula, G. Durán, A. Galembeck, K. Cogo-Müller, M. Franz-Montan, and N. Durán, 2017. Silver nanoparticles in dentistry. Dental Materials, 33(10): 1110-1126.

Omar, M.M., and H.A. Jabber, 2017. Isolation, screening and identification of Bacillus sp. producing alkaline protease. The Iraqi Journal of Agricultural Science, 48(6): 1493-1503.

Ovais, M., A.T. Khalil, A. Raza, M.A. Khan, I. Ahmad, N.U. Islam, ... and Z.K. Shinwari, 2016. Green synthesis of silver nanoparticles via plant extracts: beginning a new era in cancer theranostics. Nanomedicine, 12(23):3157-3177.

Pal, S., Y.K. Tak, and J.M. Song, 2007. Does the antibacterial activity of silver nanoparticles depend on the shape of the nanoparticle? A study of the gram-negative bacterium Escherichia coli. Applied and environmental microbiology, 73(6): 1712-1720.

Paramelle, D., A. Sadovoy, S. Gorelik, P. Free, J. Hobley, and D.G. Fernig, 2014. A rapid method to estimate the concentration of citrate capped silver nanoparticles from UV-visible light spectra. Analyst, 139(19): 4855-4861.

Park, J., D.H. Lim, H.J. Lim, T. Kwon, J.S. Choi, S. Jeong, and J. Cheon, 2011. Size dependent macrophage responses and toxicological effects of Ag nanoparticles. Chemical communications, 47(15): 4382-4384.

Parveen, R., P.K. Maiti, N. Murmu, and A. Datta, 2021. Preparation of serum capped silver nanoparticles for selective killing of microbial cells sparing host cells. Scientific Reports, 11(1): 11610.

Qing, Y.A., L. Cheng, R. Li, G. Liu, Y. Zhang, X. Tang, ... and Y. Qin, 2018. Potential antibacterial mechanism of silver nanoparticles and the optimization of orthopedic implants by advanced modification technologies. International journal of nanomedicine, 3311-3327.

Rafique, M., I. Sadaf, M.S. Rafique, and M.B. Tahir, 2017. A review on green synthesis of silver nanoparticles and their applications. Artificial cells, nanomedicine, and biotechnology, 45(7): 1272-1291.

Rai, A., A. Singh, A. Ahmad, and M. Sastry, 2006. Role of halide ions and temperature on the morphology of biologically synthesized gold nanotriangles. Langmuir, 22(2): 736-741.

Rai, M., A. Yadav, and A. Gade, 2009. Silver nanoparticles as a new generation of antimicrobials. Biotechnology advances, 27(1): 76-83.

Rao, B., and R.C. Tang, 2017. Green synthesis of silver nanoparticles with antibacterial activities using aqueous Eriobotrya japonica leaf extract. Advances in natural sciences: Nanoscience and nanotechnology, 8(1): 015014.

Rashid, M.M.O., K.N. Akhter, J.A. Chowdhury, F. Hossen, M.S. Hussain, and M.T. Hossain, 2017. Characterization of phytoconstituents and evaluation of antimicrobial activity of silver-extract nanoparticles synthesized from Momordica charantia fruit extract. BMC complementary and alternative medicine, 17(1):1-7.

Reidy, B., A. Haase, A. Luch, K.A. Dawson, and I. Lynch, 2013. Mechanisms of silver nanoparticle release, transformation and toxicity: a critical review of current knowledge and recommendations for future studies and applications. Materials, 6(6): 2295-2350.

Roy, S., and T.K. Das, 2015. Plant mediated green synthesis of silver nanoparticles-A. Int. J. Plant Biol. Res., 3:1044-1055.

Sachin, S., P. Anupama, and K. Meenal, 2012. Biosynthesis of silver nanoparticles by marine bacterium, idiomarine Sp. PR-58-5. J. Bull. Mater. Sci., 35: 1201–1205.

Saravanan, M., S. Arokiyaraj, T. Lakshmi, and A. Pugazhendhi, 2018. Synthesis of silver nanoparticles from Phenerochaete chrysosporium (MTCC-787) and their antibacterial activity against human pathogenic bacteria. Microbial pathogenesis, 117: 68-72.

Sathishkumar, M., K. Sneha, S.W. Won, C.W. Cho, S. Kim, and Y.S. Yun, 2009. Cinnamon zeylanicum bark extract and powder mediated green synthesis of nano-crystalline silver particles and its bactericidal activity. Colloids and Surfaces B: Biointerfaces, 73(2): 332-338.

Seppälä, H., T. Klaukka, J. Vuopio-Varkila, A. Muotiala, H. Helenius, K. Lager, ... and Finnish Study Group for Antimicrobial Resistance, 1997. The effect of changes in the consumption of macrolide antibiotics on erythromycin resistance in group A streptococci in Finland. New England Journal of Medicine, 337(7): 441-446.

Shaikh, S., N. Nazam, S.M.D. Rizvi, K. Ahmad, M.H. Baig, E.J. Lee, and I. Choi, 2019. Mechanistic insights into the antimicrobial actions of metallic nanoparticles and their implications for multidrug resistance. International journal of molecular sciences, 20(10): 2468.

Sharma, V.K., R.A. Yngard, and Y. Lin, 2009. Silver nanoparticles: green synthesis and their antimicrobial activities. Advances in colloid and interface science, 145(1-2): 83-96.

Shivaji, S., S. Madhu, and S. Singh, 2011. Extracellular synthesis of antibacterial silver nanoparticles using psychrophilic bacteria. Process Biochemistry, 46(9): 1800-1807.

Singh, J., G. Kaur, P. Kaur, R. Bajaj, and M. Rawat, 2016. A review on green synthesis and characterization of silver nanoparticles and their applications: a green nanoworld. World J. Pharm. Pharm. Sci., 6(7).

Singh, P., and I. Mijakovic, 2022. Antibacterial effect of silver nanoparticles is stronger if the production host and the targeted pathogen are closely related. Biomedicines, 10(3): 628.

Sivaraman, D., P. Panneerselvam, P. Muralidharan, T.P. Prabhu, and R.V. Kumar, 2013. Green synthesis, characterization and anti-microbial activity of silver nanoparticles produced using Ipomoea aquatica forsk leaf extract. International Journal of Pharmaceutical Sciences and Research, 4(6): 2280.

Sonnenwirth, A.C., 1972. Evolution of anaerobic methodology. The American Journal of Clinical Nutrition, 25(12): 1295-1298.

Suaya, J.A., R.M. Mera, A. Cassidy, P. O'Hara, H. Amrine-Madsen, S. Burstin, and L.G. Miller, 2014. Incidence and cost of hospitalizations associated with Staphylococcus aureus skin and soft tissue infections in the United States from 2001 through 2009. BMC infectious diseases, 14:1-8.

Wahab, S., T. Khan, M. Adil, and A. Khan, 2021. Mechanistic aspects of plant-based silver nanoparticles against multi-drug resistant bacteria. Heliyon, 7(7).

Wayne, P.A., 2005. Clinical and laboratory standards institute; 2007. Performance standards for antimicrobial susceptibility testing. CLSI document M100-S17.

Wiegand, I., K. Hilpert, and R.E. Hancock, 2008. Agar and broth dilution methods to determine the minimal inhibitory concentration (MIC) of antimicrobial substances. Nature protocols, 3(2): 163-175.

Winn, W.C., S. Allen, W.M. Janda, E.W. Koneman, P.C. Schreckenberger, G. Procop, and G. Baker Woods, 2006. Miscellaneous fastidious gram-negative bacilli. Koneman's Color Atlas and Textbook of Diagnostic Microbiology, 6th edition, Philadelphia, PA, Lippincott, Williams and Wilkins, 472-473.

Xiu, Z.M., Q.B. Zhang, H.L. Puppala, V.L. Colvin, and P.J. Alvarez, 2012. Negligible particle-specific antibacterial activity of silver nanoparticles. Nano letters, 12(8): 4271-4275.

Xu, L., Y.Y. Wang, J. Huang, C.Y. Chen, Z.X. Wang, and H. Xie, 2020. Silver nanoparticles: Synthesis, medical applications and biosafety. Theranostics, 10(20): 8996.

Yin, I.X., J. Zhang, I.S. Zhao, M.L. Mei, Q. Li, and C.H. Chu, 2020. The antibacterial mechanism of silver nanoparticles and its application in dentistry. International journal of nanomedicine, 2555-2562.